

# Integration of Coherence and Volumetric Curvature Attributes\*

Satinder Chopra<sup>1</sup> and Kurt J. Marfurt<sup>2</sup>

Search and Discovery Article #40770 (2011)

Posted July 18, 2011

\*Adapted from oral presentation at AAPG Annual Convention and Exhibition, Houston, Texas, USA, April 10-13, 2011.

<sup>1</sup>Arcis Corporation, Calgary, AB, Canada. ([schopra@arcis.com](mailto:schopra@arcis.com))

<sup>2</sup>University of Oklahoma, Norman, OK.

## Abstract

Volumetric curvature is a well-established interpretational tool that allows us to image subtle faults, folds, incised channels, differential compaction, and a wide range of other stratigraphic features. In general, curvature is an excellent measure of paleo-deformation. With an appropriate tectonic deformation model, a good structural geologist can predict where fractures were formed. However, since their formation, such fractures may have been cemented, filled with overlying sediments or diagenetically altered. Furthermore, the present-day direction of minimum horizontal stress may have rotated from the direction at the time of deformation, such that previously open fractures are now closed, while previously closed fractures may now be open. For this reason, prediction of open fractures requires not only images of faults and flexures provided by coherence and curvature coupled with an appropriate model of deformation, but also measures of present day stress provided by breakouts seen in image lots and seismic anisotropy measures.

The maximum and minimum curvatures (and two principal curvatures),  $k_{\max}$  and  $k_{\min}$ , define the eigenvalues of a quadratic surface, while the azimuth of minimum curvature,  $\psi_{\min}$ , defines the eigenvectors projected onto the horizontal plane. By definition (and based on eigenstructure analysis), the maximum curvature is defined as the principal curvature that has the larger absolute value. However, we find that the principal curvatures  $k_1$  and  $k_2$ , where  $k_1 \geq k_2$ , provide the simplicity of interpretation seen in  $k_{\text{pos}}$  and  $k_{\text{neg}}$ , but retain the robustness of  $k_{\max}$  and  $k_{\min}$  in the presence of steep dip. In the case of faults and folds, a cursory look at the horizon slices through the most-positive curvature,  $k_{\text{pos}}$ , and the most-positive principal curvature  $k_1$  show longer, more continuous folds and flexures, which continue even where their absolute value is less than that of  $k_{\text{neg}}$  or  $k_2$ . For this reason, many authors favor these displays when mapping stratigraphic features as well as subtle faults and fractures in the presence of gentle dip. However, in areas of folding in the presence of significant dip, the crest and trough

of a fold defined as the highest and lowest points on a vertical section no longer correspond to the locations of the tightest folding. We will illustrate these conclusions with real data examples.

### **Selected References**

Al-Dossary, S., and K.J. Marfurt, 2006, 3D volumetric multispectral estimates of reflector curvature and rotation: *Geophysics*, v. 71/5, p. P41-P51.

Bakker, P., 2003, Image structure analysis for seismic interpretation: Ph.D. Thesis, Technisch Universiteit Delft, Netherlands, 130 p.

Blumentritt, C.H., and B. Stinson, 2006, Volume based curvature analysis illuminates fracture orientations, Fort Worth Basin, Texas, *in* Anonymous (ed.) AAPG 2006 Annual Convention Abstracts, v. 15, p. 11-12.

Fomel, S., 2008, Predictive painting of 3D seismic volumes: 77<sup>th</sup> Annual International Meeting of the SEG, Expanded Abstracts, p. 864-868.

Hart, B.S., R. Pearson, R. Pearson, and G.C. Rawling, 2002, 3-D seismic horizon-based approaches to fracture-swarm sweet spot definition in tight-gas reservoirs: *The Leading Edge*, v. 21, p. 28-35.

Hart, M.B., 2003, The search for the origin of the planktic Foraminifera: *Journal of the Geological Society*, v. 160, p. 341-343.

Lisle, R.J., 1994, Detection of zones of abnormal strains in structures using Gaussian curvature analysis: *AAPG Bulletin*, v. 78/12, p. 1811-1819.

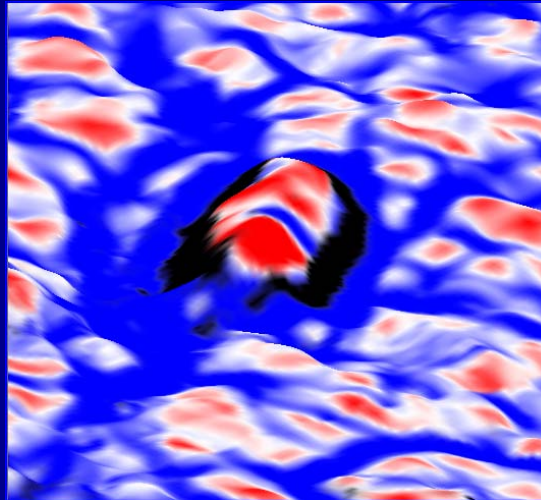
Marfurt, K.J., 2006, Robust estimates of reflector dip and azimuth: *Geophysics*, v. 71, p. p. 29-40.

Rich, J., 2008, Expanding the applicability of curvature attributes through clarification of ambiguities in derivation and terminology: 77<sup>th</sup> Annual Meeting of the SEG, p. 884-887.

Roberts, A., 2001, Curvature attributes and their application to 3D interpreted horizons: *First Break*, v. 19, p. 85-99.

Sigismondi, E.M., and C.J. Soldo, 2003, Curvature attributes and seismic interpretation: Case studies from Argentina basins: The Leading Edge, v. 22, p. 1122-1126.

# Integration of coherence and volumetric curvature images



*Satinder Chopra\**



**ARCIS CORPORATION,  
CALGARY**

*and*

*Kurt Marfurt*



**UNIVERSITY OF OKLAHOMA,  
NORMAN**

# Integration of coherence and volumetric curvature images

- Volumetric discontinuity attributes are powerful tools in the detection of stratigraphic features or prediction of fractures.
- Geologic structures often exhibit curvature of different wavelengths. Curvature images having different wavelength provide different perspectives of the same geology.
- Tight curvature often delineates details within intense, highly localized fracture systems.
- Broad curvature often enhances subtle flexures on the scale of 100-200 traces that are difficult to see on conventional seismic. However, these are correlated to fracture zones that are below seismic resolution, as well as collapse features and diagenetic alterations.
- Multi-spectral volumetric estimates of curvature are very useful for seismic interpreters and we are going to see some examples demonstrating this.

# Integration of coherence and volumetric curvature images

- Initial curvature applications were limited to picked horizons on 3D seismic volumes.
- These applications include:
  - Delineating faults (Sigismondi and Soldo, 2003)
  - Subtle carbonate buildups (Hart, 2003)
  - Correlation to open fractures measured on outcrops (Lisle, 1994)
  - Correlation to open fractures to production data (Hart et al, 2002)
- Horizon-based curvature is limited by:
  - Interpreter's ability to pick horizons
  - Existence of horizons of interest at the appropriate level, which could be a challenge if rock interfaces do not exhibit consistent impedance contrast.
  - The noise in the data.

# Integration of coherence and volumetric curvature images

- This issue was addressed by volumetric curvature introduced by Al-Dossary and Marfurt (2006).
  - Volumetric estimates of curvature are generated from volumetric estimates of reflector dip and azimuth, which could be calculated in different ways:
    - Using complex traces analysis (Barnes, 2000)
    - Gradient structure tensor (Bakker, 2003)
    - Discrete semblance-based searches (Marfurt, 2006)
    - Plane-wave destructor techniques (Fomel, 2008)
  - There are many different types of curvature that can be computed and several authors have found a good correlation between:
    - Dip curvature
    - Strike curvature (Hart et al, 2002)
    - Gaussian curvature (Lisle, 1994)
- and open fractures

# Integration of coherence and volumetric curvature images

- In general, curvature is a good measure of paleo deformation.
- With an appropriate tectonic deformation model, a good structural geologists can predict where fractures were formed.
- However, since their formation, such-fractures have been:
  - Cemented (Rich, 2008)
  - Filled with overlying sediments (Nissen, 2006)
  - Diagenetically altered (Nissen, 2007)
- In addition to all this, the present-day direction of minimum horizontal stress may have been rotated from the direction at the time of deformation, so that previously open fractures are now closed and the previously closed fractures are now open.

Consequently, prediction of open fractures requires not only images of faults and flexures provided by coherence and curvature, coupled with an appropriate model of deformation, but also measures of present day stress provided by breakouts seen in image logs and seismic anisotropy measures.

# Integration of coherence and volumetric curvature images

- As mentioned before, there are various curvature measures. Different workers have used maximum and minimum curvature measures.
- Most of the work on curvature attribute applications that we have published, has been on the application of most-positive and most-negative curvature attributes.
- In this talk we are going to, amongst other things, also propose the use of principal maximum and minimum curvature measures.
- Finally, we are going to show a number of applications of different curvature measures and the integration of coherence and curvature measures.

# Integration of coherence and volumetric curvature images

➤ Curvature of a 2D surface (Sigismondi and Soldo, 2003)

$$k_{2D} = \frac{1}{R} = \frac{\frac{d^2 z}{dx^2}}{\left[1 + \left(\frac{dz}{dx}\right)^2\right]^{3/2}} \quad (1)$$

where R is the radius of curvature and  $z(x)$  is the elevation of a 2D horizon.

2D curvature is defined as the change in the radius of curvature, and hence of the angle of the normal with the vertical,  $\varphi = \tan^{-1}(z/x)$ .

# Integration of coherence and volumetric curvature images

➤ From our lessons in calculus

$$c_{2D} = \frac{d^2 z}{dx^2} \quad (2)$$

Sigismondi and Soldo (2003) show that the peak values of equation 2 will occur at the crest of a folded 2D image, while the peak values of equation 1 will occur at the position of tightest curvature having a positive value.

# Integration of coherence and volumetric curvature images

In 3D, we encounter somewhat more difficult to visualize formulae. We use Roberts (2001) notation and assume we fit a picked horizon with a quadratic surface of the form:

$$z(x,y) = ax^2 + cxy + by^2 + dx + ey + f.$$

Roberts (2001) then goes on to define the mean curvature,  $k_{mean}$ , Gaussian curvature,  $k_{Gauss}$ , and principal curvatures,  $k_1$  and  $k_2$ :

$$k_{mean} = [a(1+e^2) + b(1+d^2) - cde] / (1+d^2+e^2)^{3/2},$$

$$k_{Gauss} = (4ab - c^2) / (1+d^2+e^2)^2,$$

$$k_1 = k_{mean} + (k_{mean}^2 - k_{Gauss})^{1/2},$$

$$k_2 = k_{mean} - (k_{mean}^2 - k_{Gauss})^{1/2},$$

Note that  $k_1$  is a *signed value* that is always greater than or equal to  $k_2$ .

## Integration of coherence and volumetric curvature images

For this reason, Roberts (2001) uses the classical definition of the maximum and minimum curvatures,  $k_{max}$  and  $k_{min}$

$$k_{max} = \begin{cases} k_1 & \text{if } |k_1| \geq |k_2| \\ k_2 & \text{if } |k_1| < |k_2| \end{cases}, \text{ and}$$
$$k_{min} = \begin{cases} k_2 & \text{if } |k_1| \geq |k_2| \\ k_1 & \text{if } |k_1| < |k_2| \end{cases}.$$

While these formulae are a 3D generalization of equation 1, it causes considerable confusion for those of us who come from a geology vs. mathematics background.

First, the maximum curvature will not always have a positive value.

If we have an elongated synclinal bowl, the maximum curvature will actually be the curvature of the shortest cross section, while the minimum curvature will be the curvature in the strike direction of our basin.

# Integration of coherence and volumetric curvature images

Several authors (including many of our publications) have favored using the most-positive,  $k_{pos}$ , and most-negative curvature  $k_{neg}$ :

$$k_{pos} = (a+b) + [(a-b)^2 + c^2]^{1/2}, \text{ and}$$

$$k_{neg} = (a+b) - [(a-b)^2 + c^2]^{1/2}.$$

For relatively flat dips, such as encountered in the Fort Worth Basin and Permian Basins of Texas (Al-Dossary and Marfurt, 2006; Blumentritt et al., 2006)  $k_{pos} \approx k_1$  and  $k_{neg} \approx k_2$ .

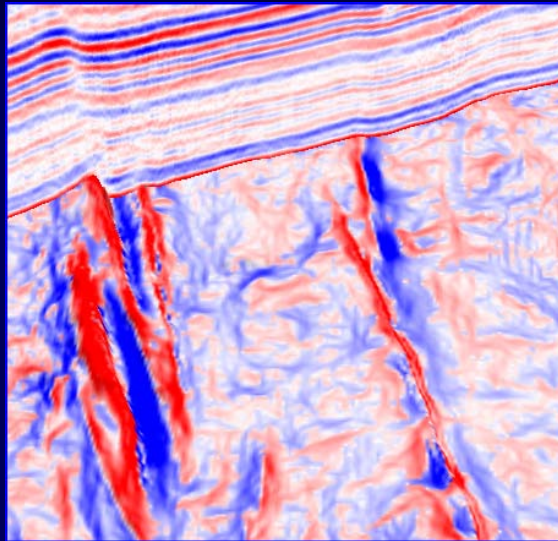
In highly deformed areas such as the deeper Chicotepec Basin of Mexico (Mai et al., 2009) the differences can be significant. By using the principal curvatures  $k_1$  and  $k_2$ , we maintain the accuracy for highly deformed terrains of  $k_{max}$  and  $k_{min}$ , while providing the interpretational simplicity of  $k_{pos}$  and  $k_{min}$ .

We also hope to eliminate the confusion on the definition of  $k_{max}$  and  $k_{min}$ , with several commercial software vendors implementing them not as defined by Roberts (2001) and the mathematical literature, but rather as we have defined  $k_1$  and  $k_2$ .

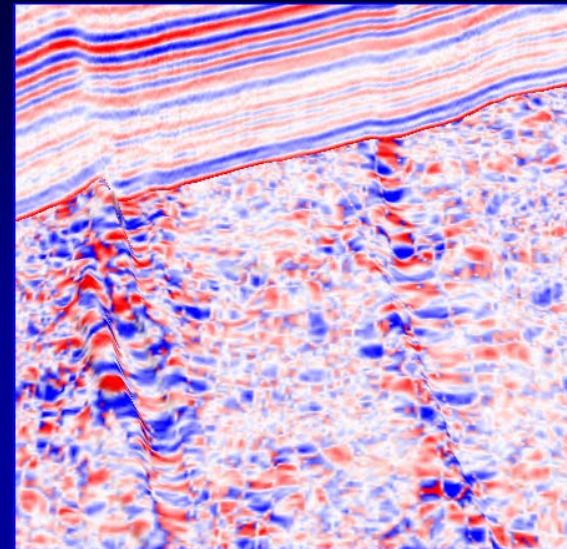
# Integration of coherence and volumetric curvature images

## Examples

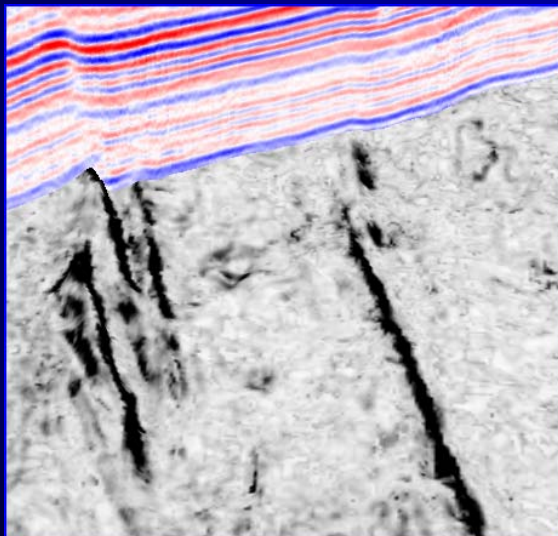
( $k_{\max}$ )



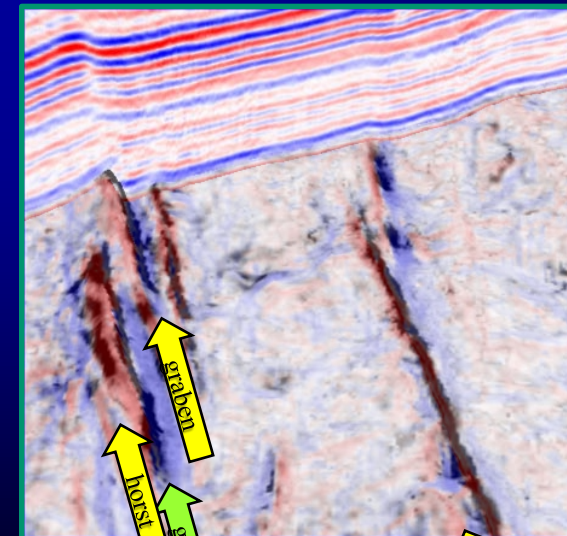
( $k_{\min}$ )



(coherence)

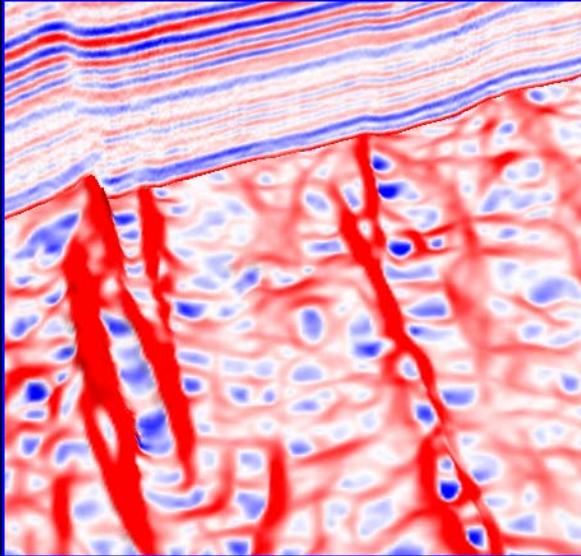


(coherence +  $k_{\max}$ )

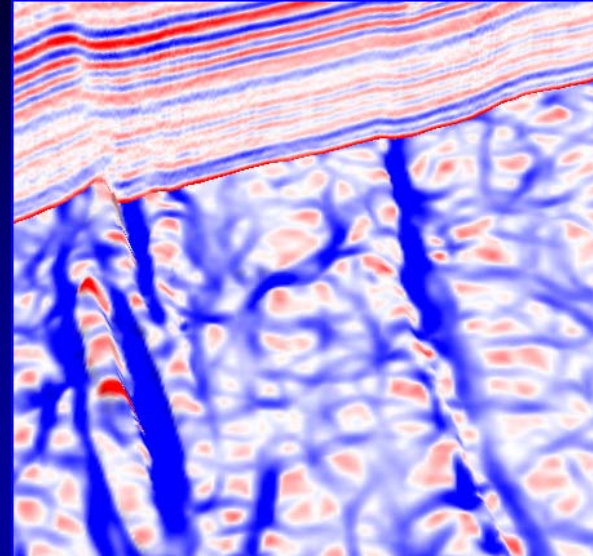


# Integration of coherence and volumetric curvature images

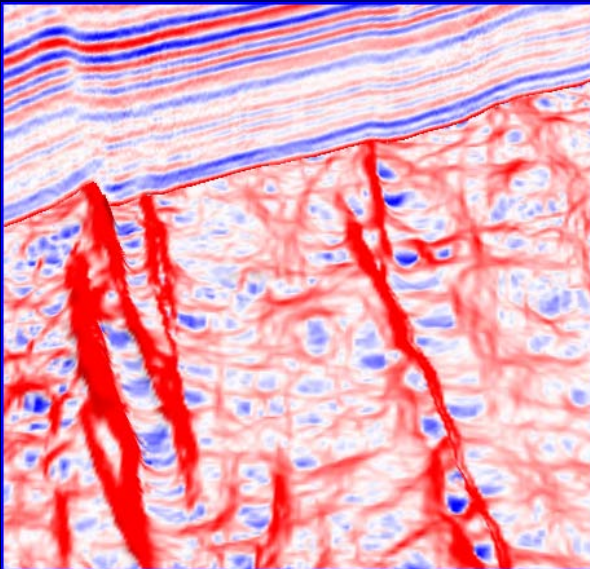
## Examples



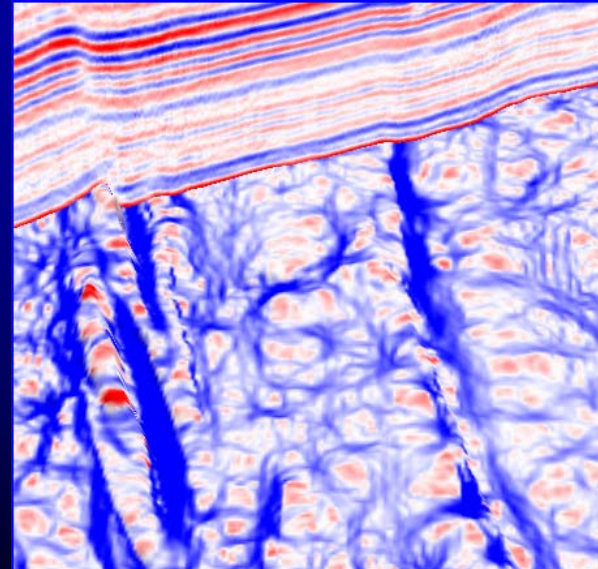
(Most-positive curvature (long-wavelength))



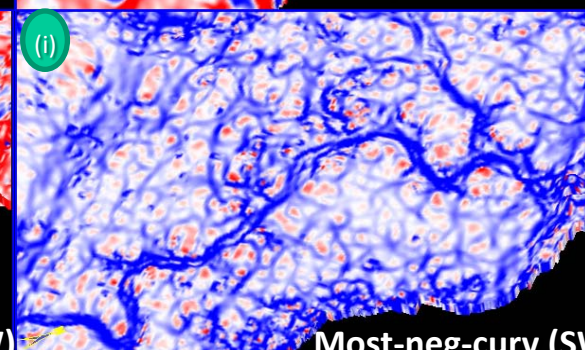
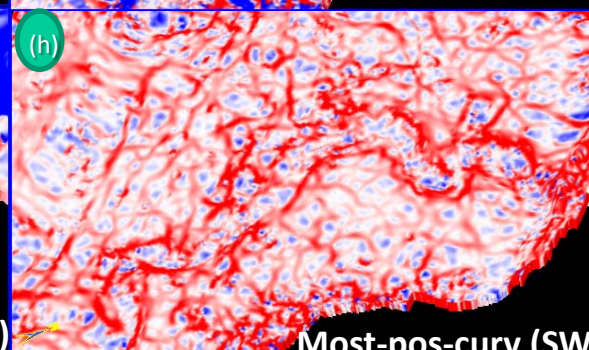
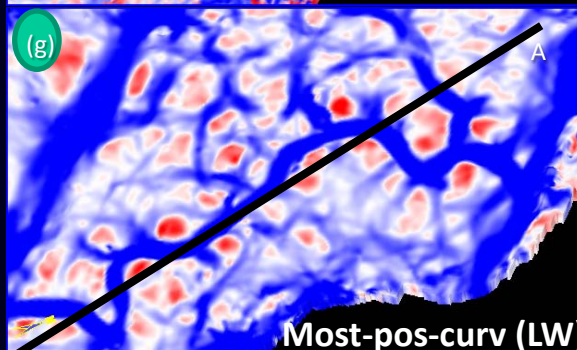
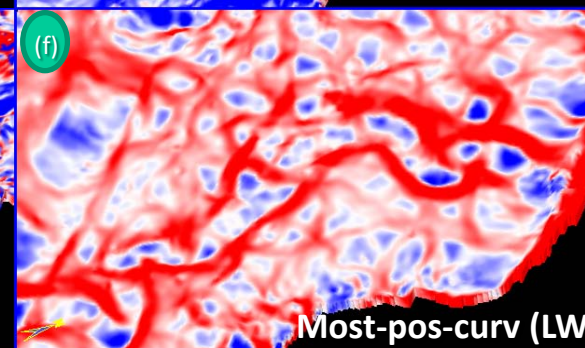
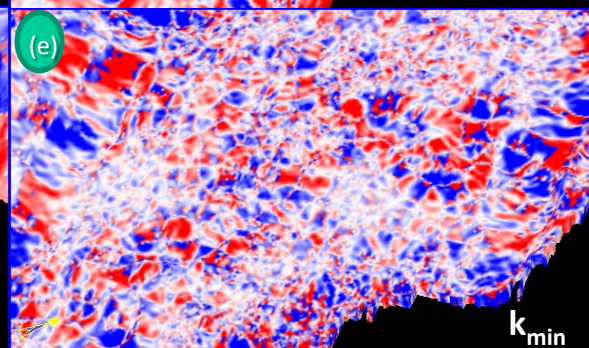
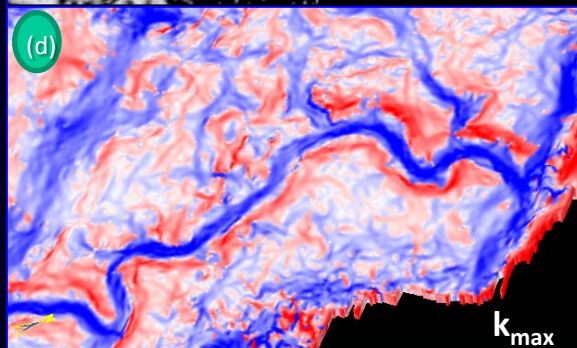
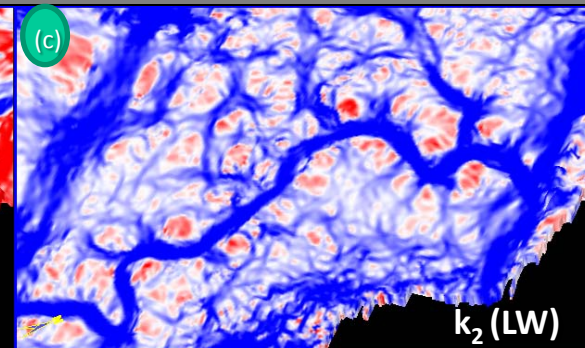
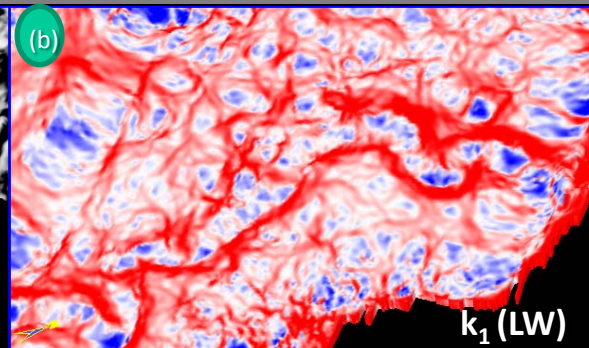
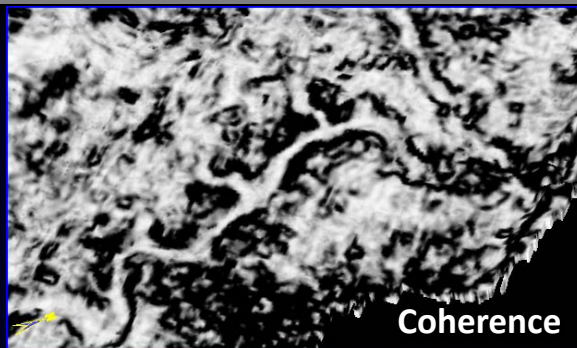
(Most-negative curvature (long-wavelength))



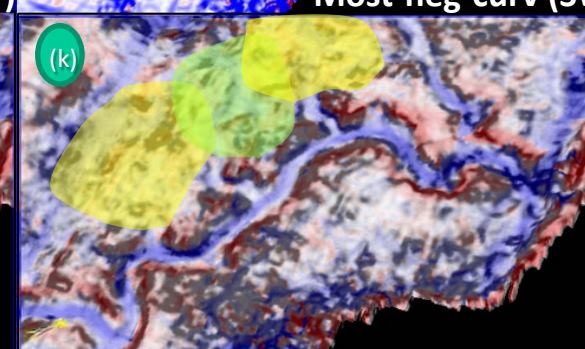
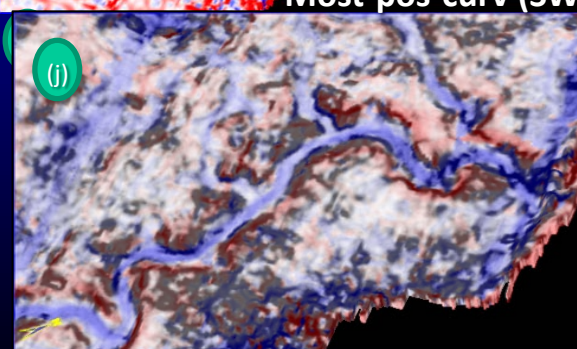
(k1 principal positive curvature (long-wavelength))



(k1 principal negative curvature (long-wavelength))



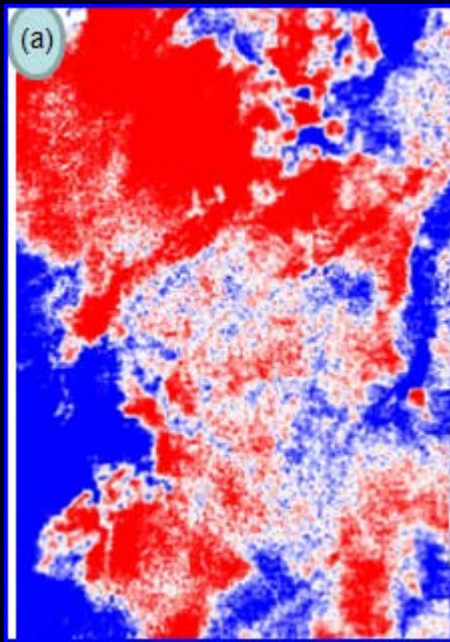
Co-rendered coherence + max-curv



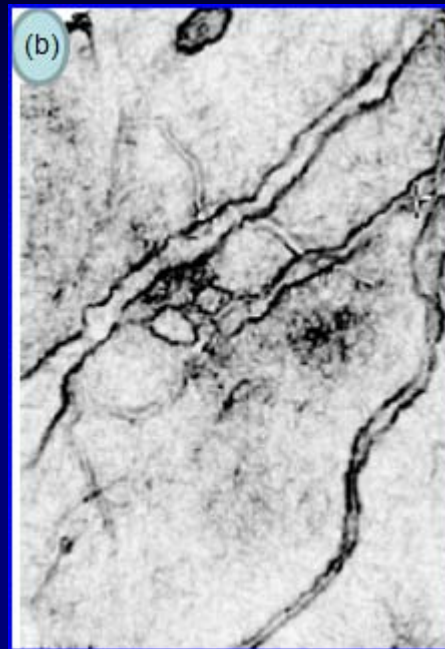
We interpret a main channel and at least three crevasse-splay features resulting in planar to slightly positive fan features.

# Integration of coherence and volumetric curvature images

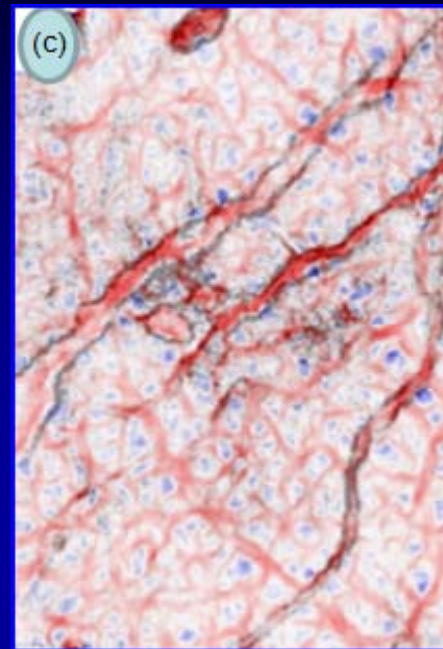
Time slices at 1096 ms



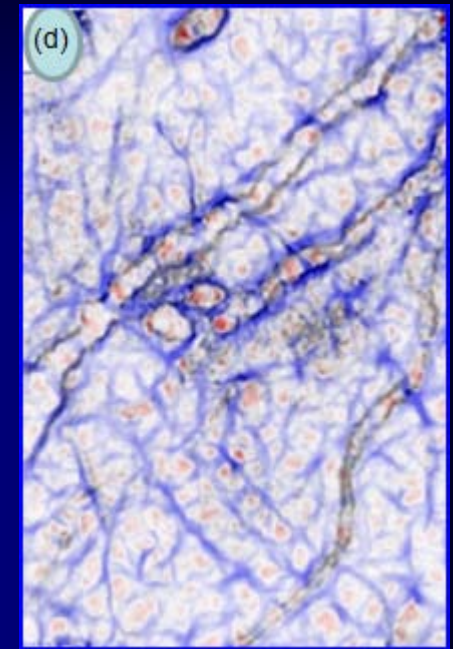
Neg 0 Pos  
Seismic



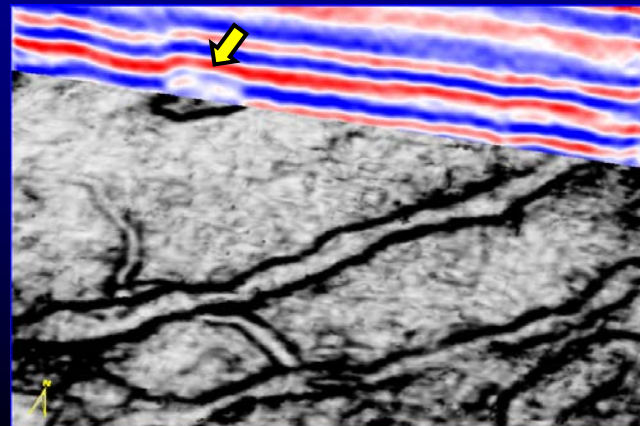
Low High  
Coherence



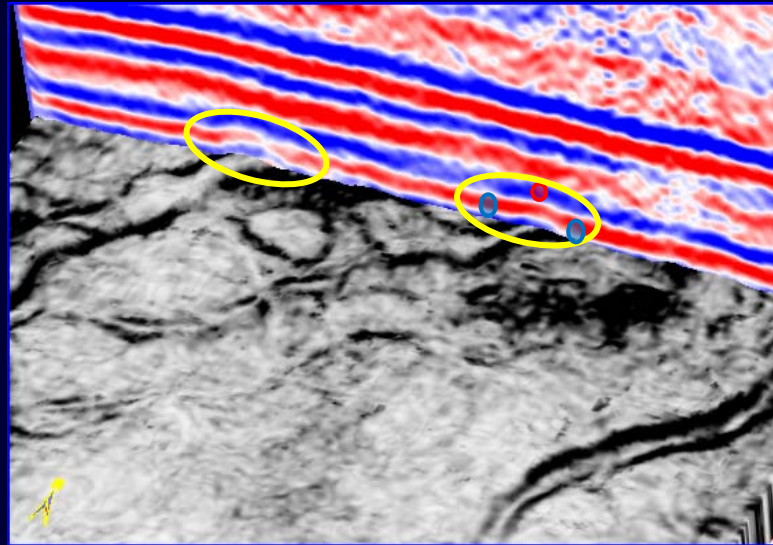
$k_1$  co-rendered with  
coherence



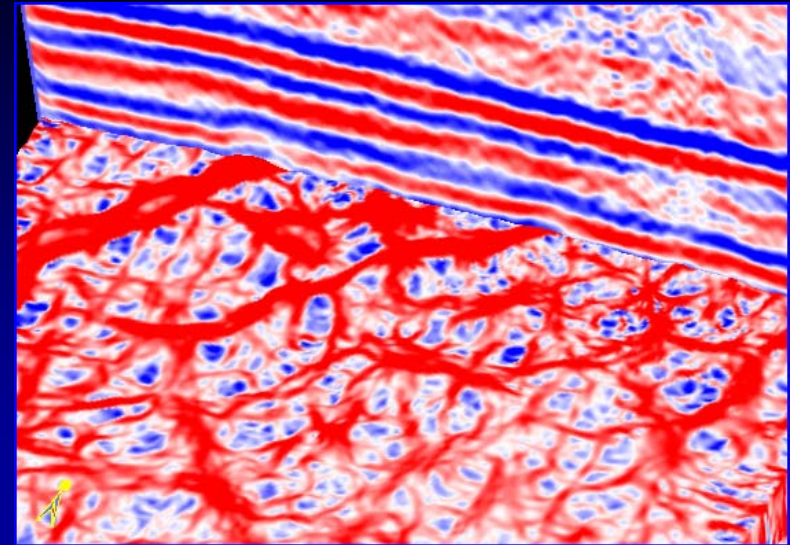
$k_2$  co-rendered with  
coherence



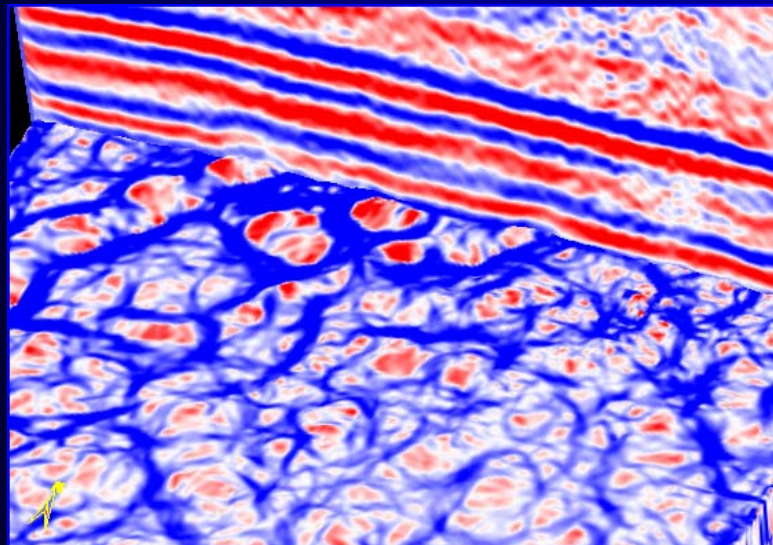
# Integration of coherence and volumetric curvature images



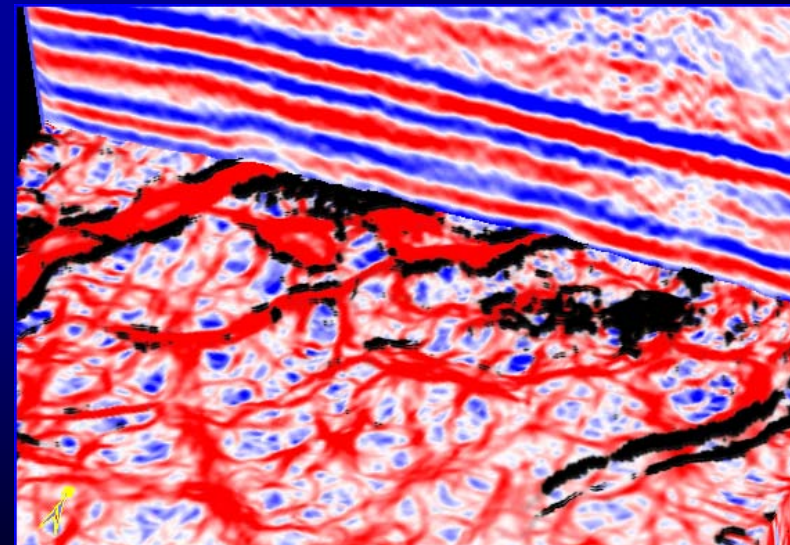
Coherence



$k_1$  (LW)



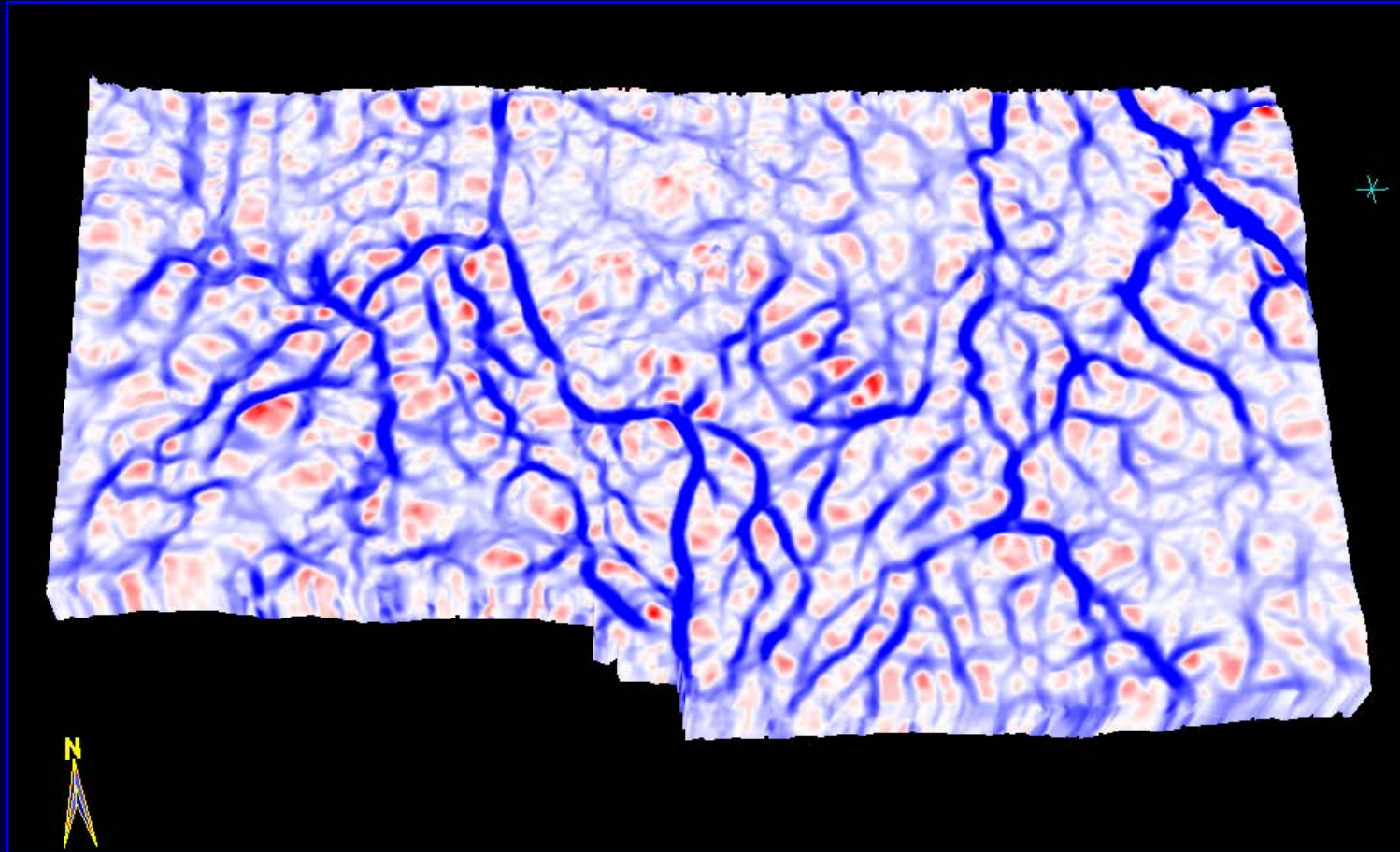
$k_2$  (LW)



$k_1$  co-rendered with coherence

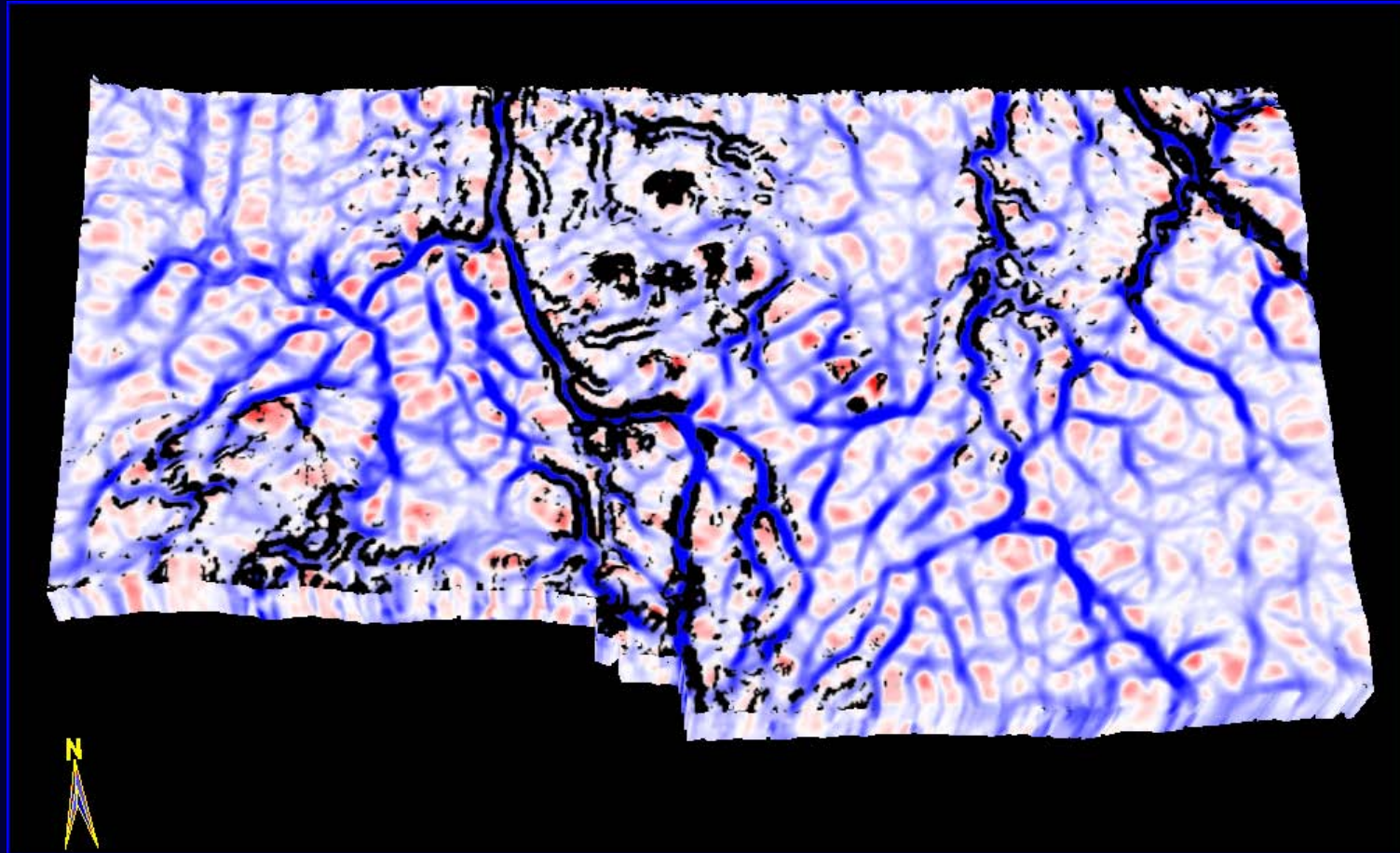
Chair displays for seismic and curvature attributes

# Integration of coherence and volumetric curvature images



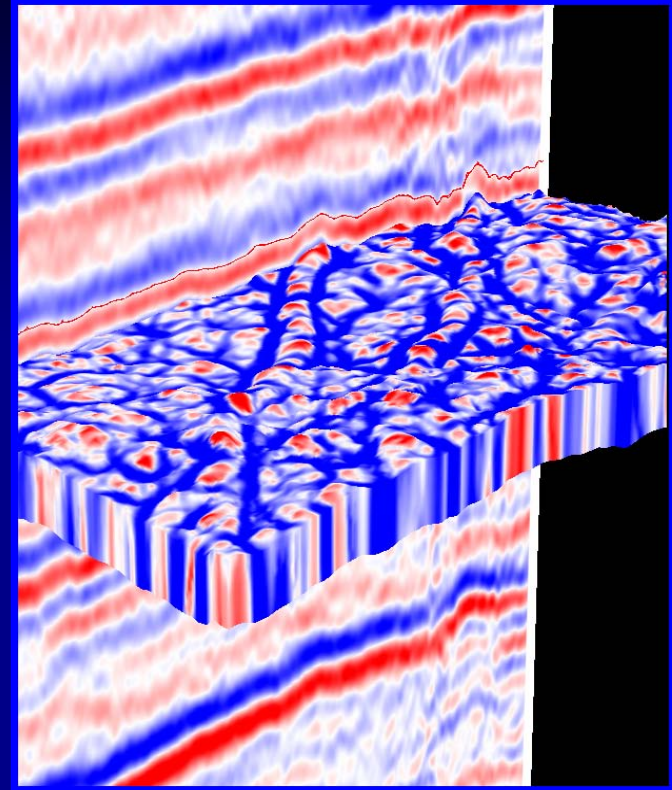
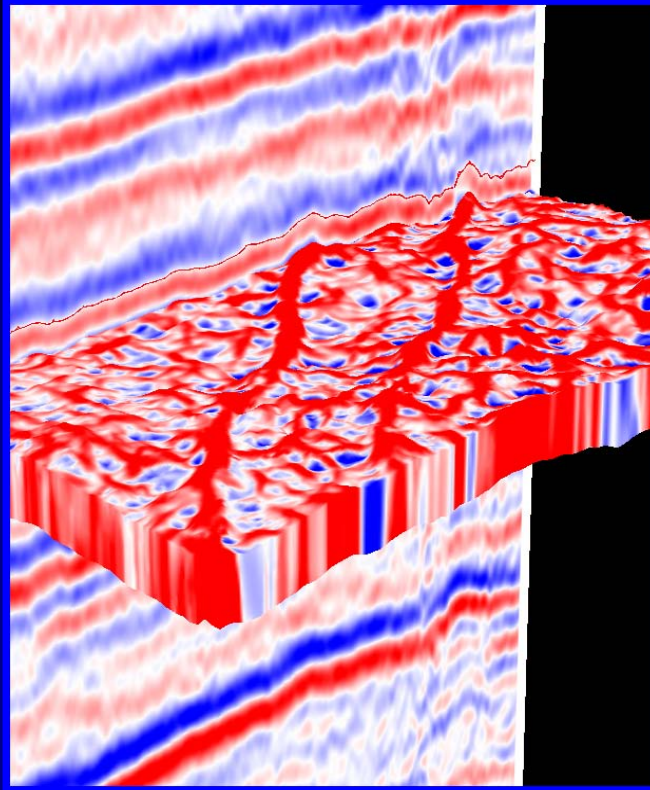
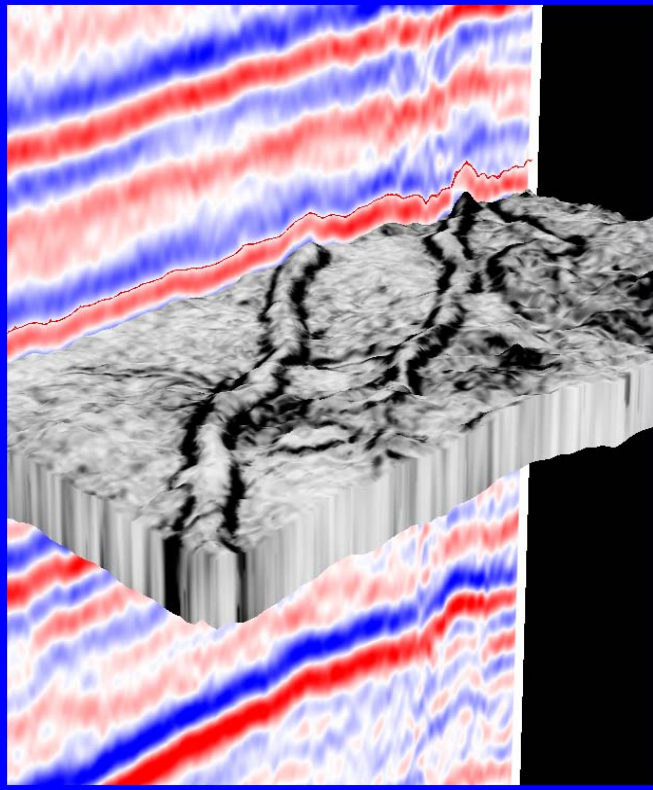
Strat-cube from most-negative curvature volume

# Integration of coherence and volumetric curvature images



Strat-cube from most-negative curvature volume co-rendered with coherence

# Integration of coherence and volumetric curvature images

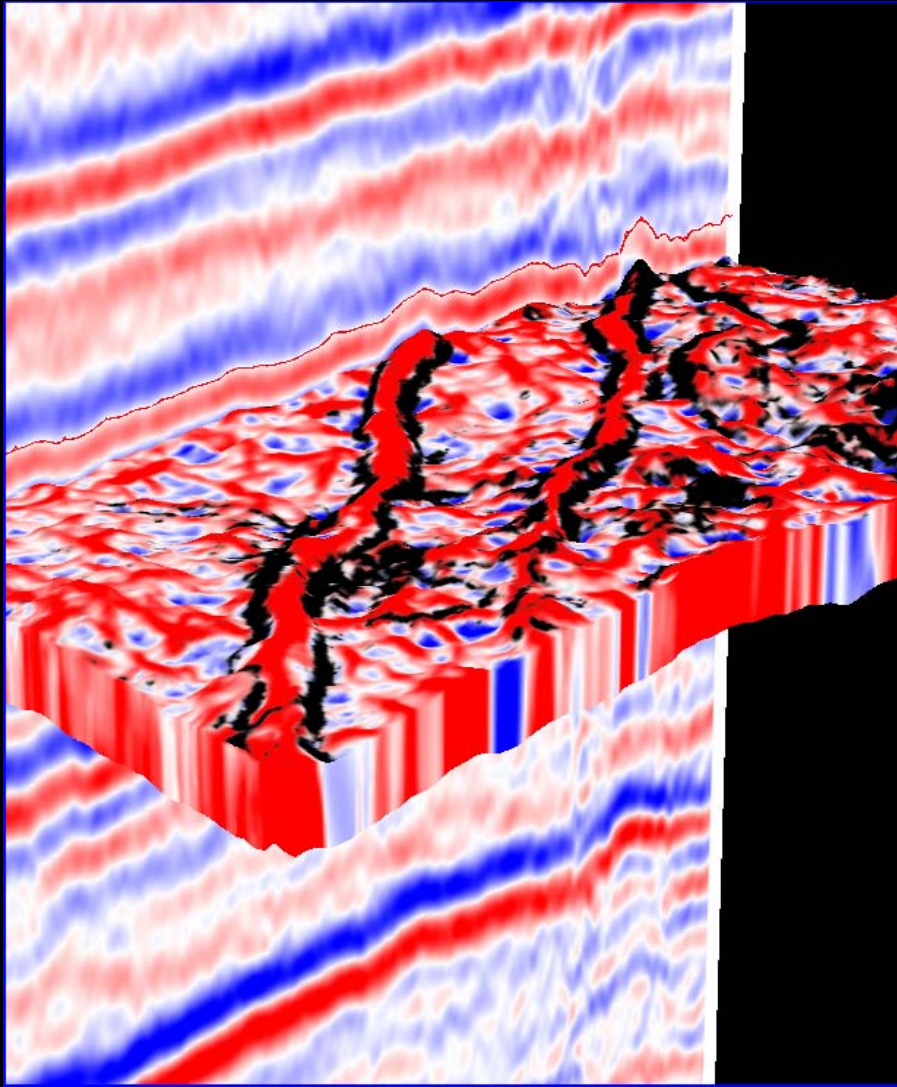


Strat-cube from the coherence attribute seen here in a 3D chair view

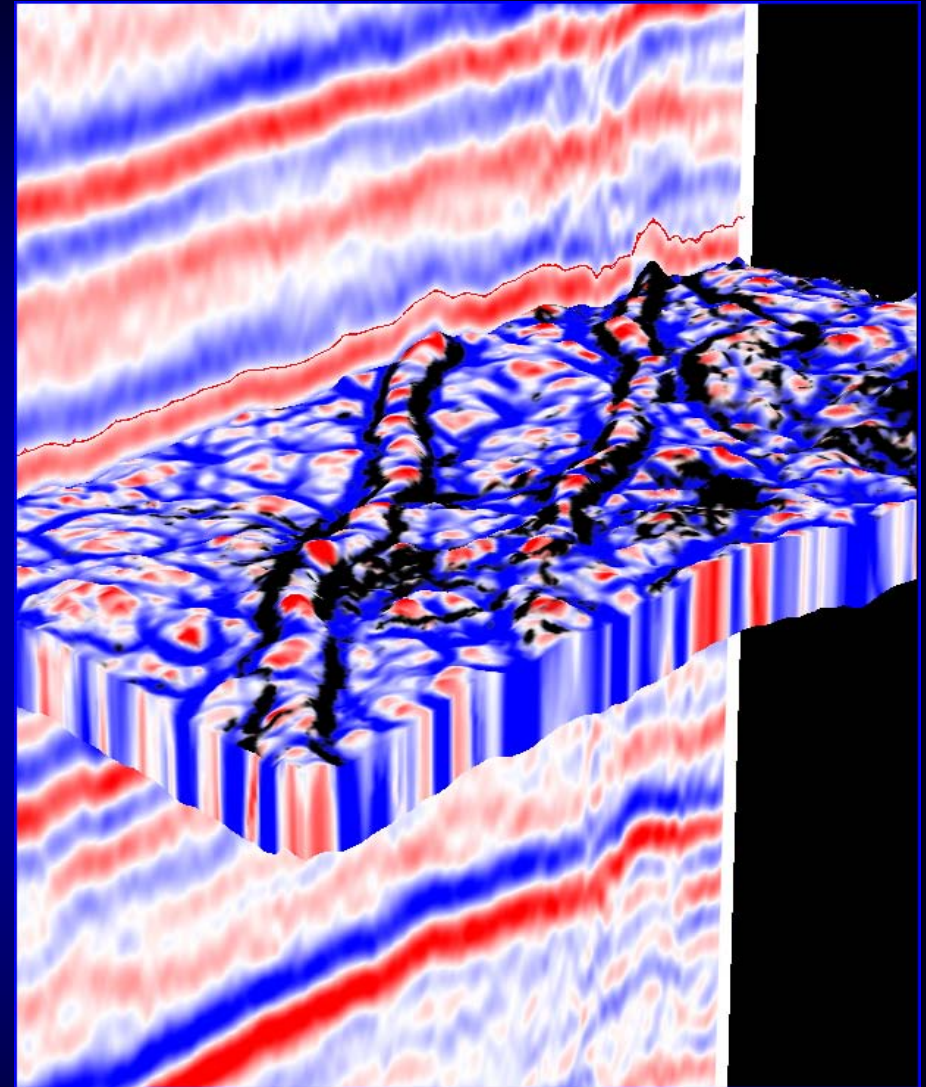
Strat-cube from the most-positive curvature attribute seen here in a 3D chair view

Strat-cube from the most-negative curvature attribute seen here in a 3D chair view

# Integration of coherence and volumetric curvature images

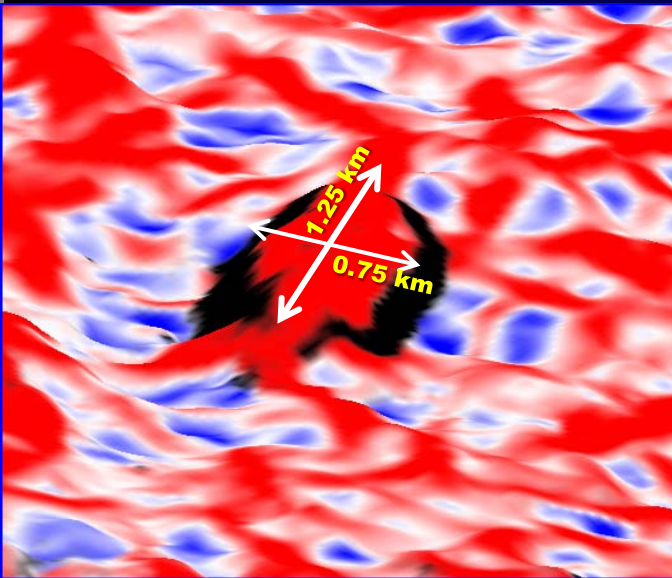


Strat-cube from the most-positive curvature attribute co-rendered with coherence seen here in a 3D chair view

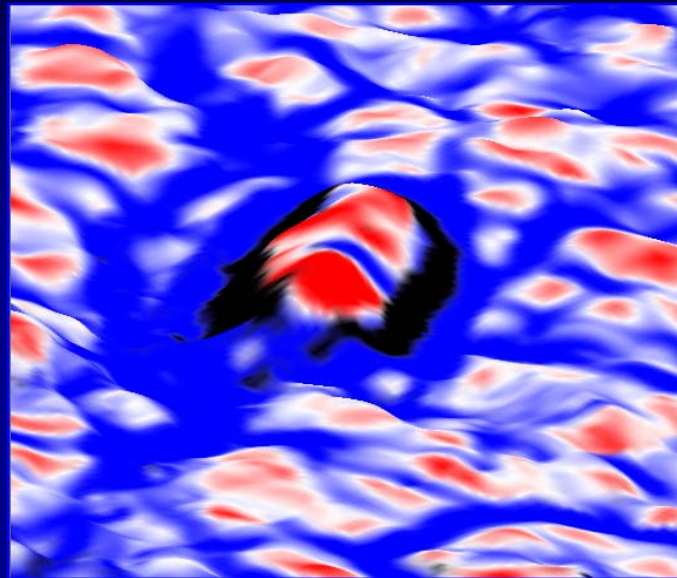


Strat-cube from the most-negative curvature attribute co-rendered with coherence seen here in a 3D chair view

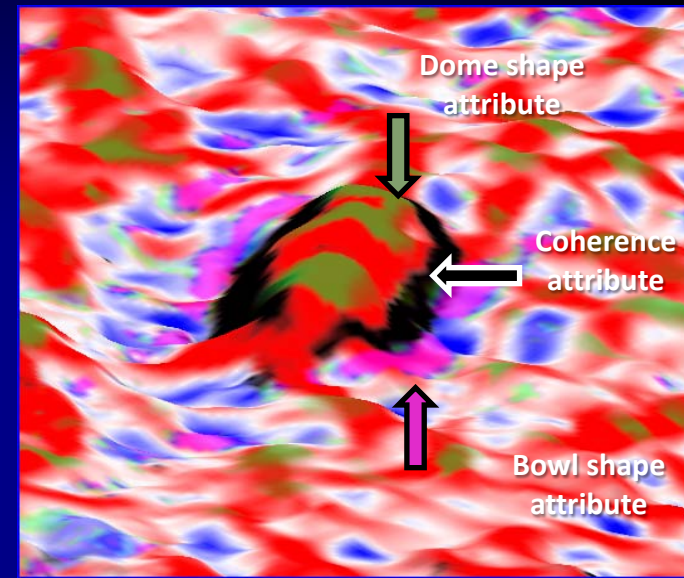
# Integration of coherence and volumetric curvature images



Strat-slice from k1 curvature co-rendered with coherence shown here in a 3D view

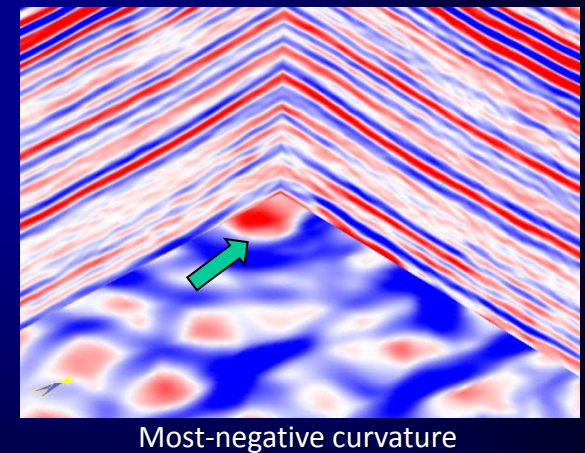
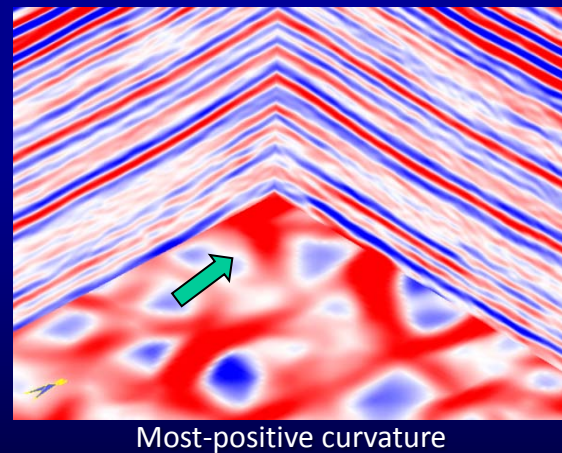
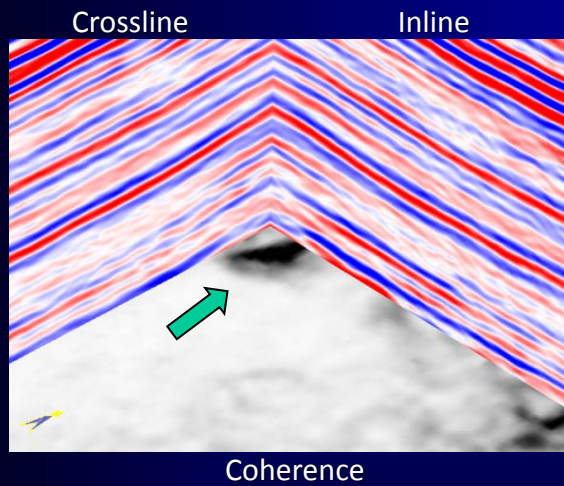
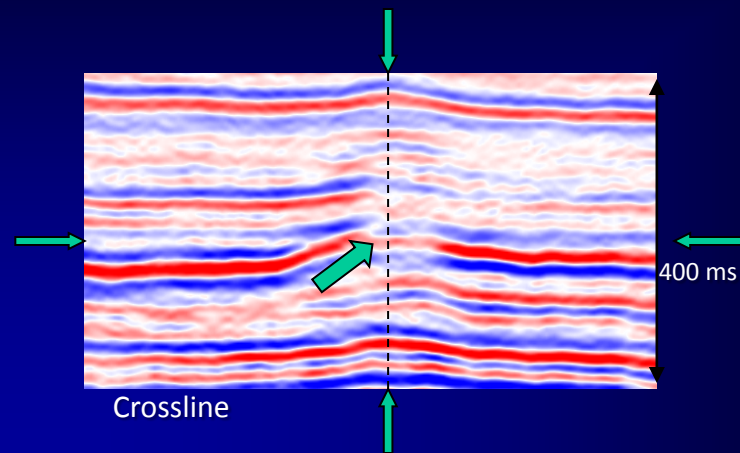
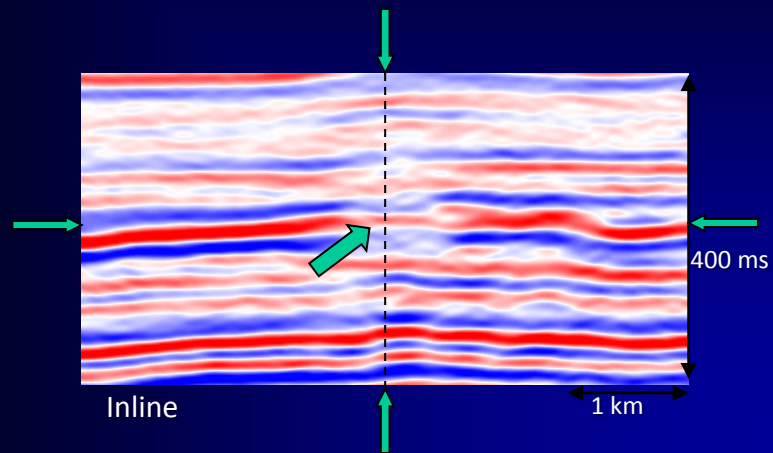


Strat-slice from k2 curvature co-rendered with coherence

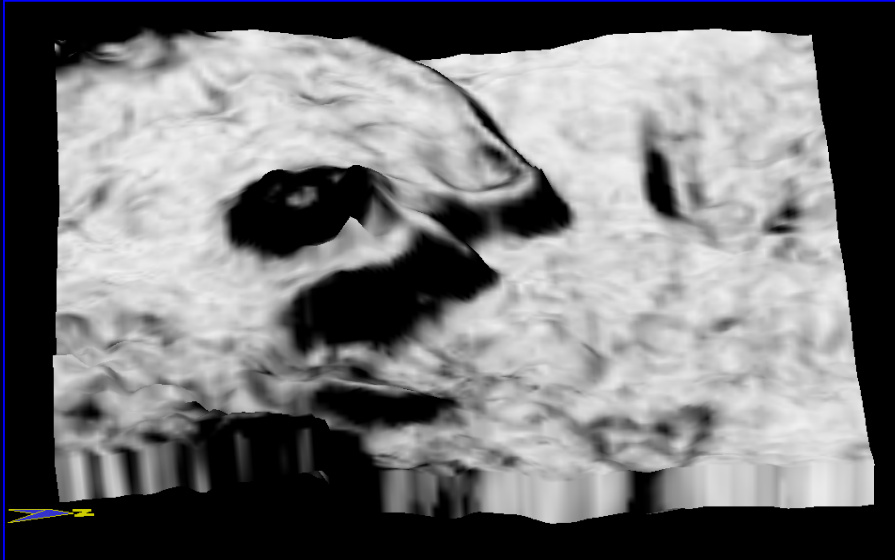


Strat-slice from k1 curvature co-rendered with coherence, bowl and dome shape attributes. The coherence, bowl and dome attributes have been displayed using transparency displaying only the values of interest.

# Integration of coherence and volumetric curvature images

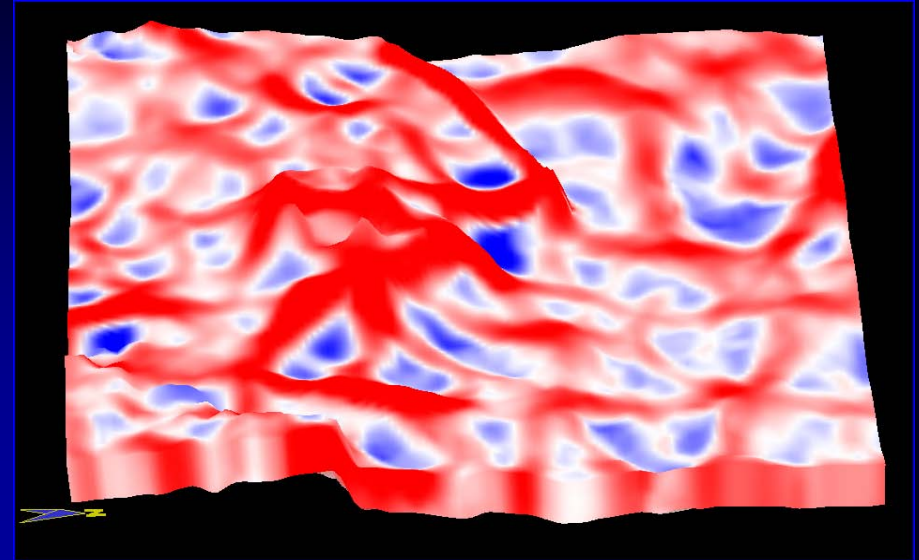


# Integration of coherence and volumetric curvature images



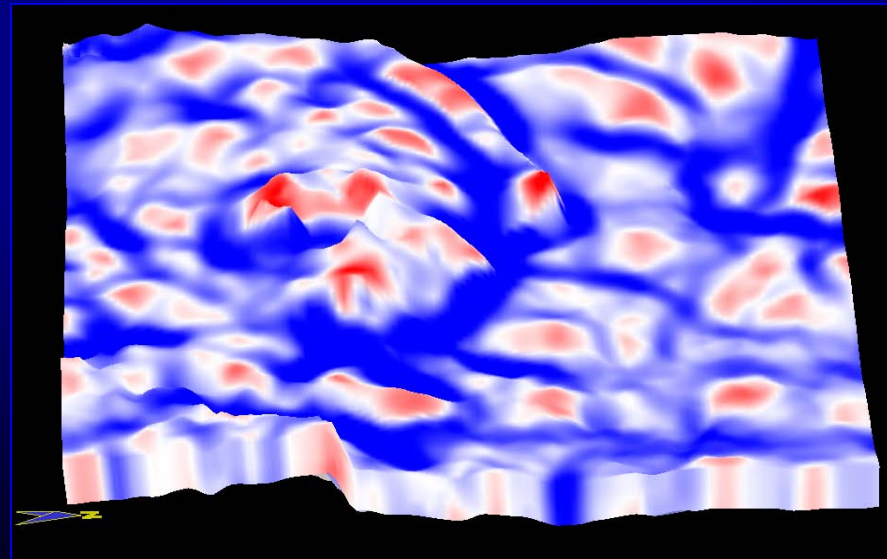
Low High

Strat-cube from coherence volume



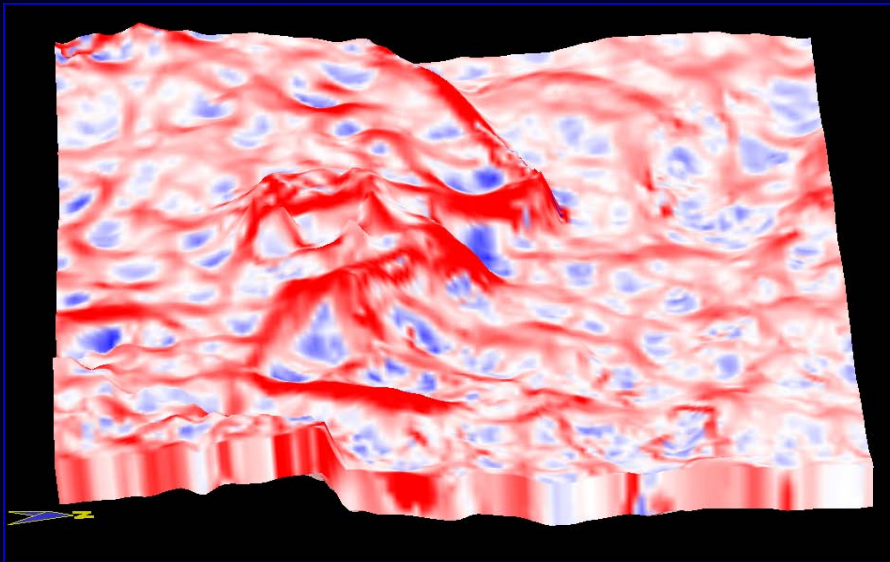
Low High

Strat-cube from most-positive curvature volume (low-res)

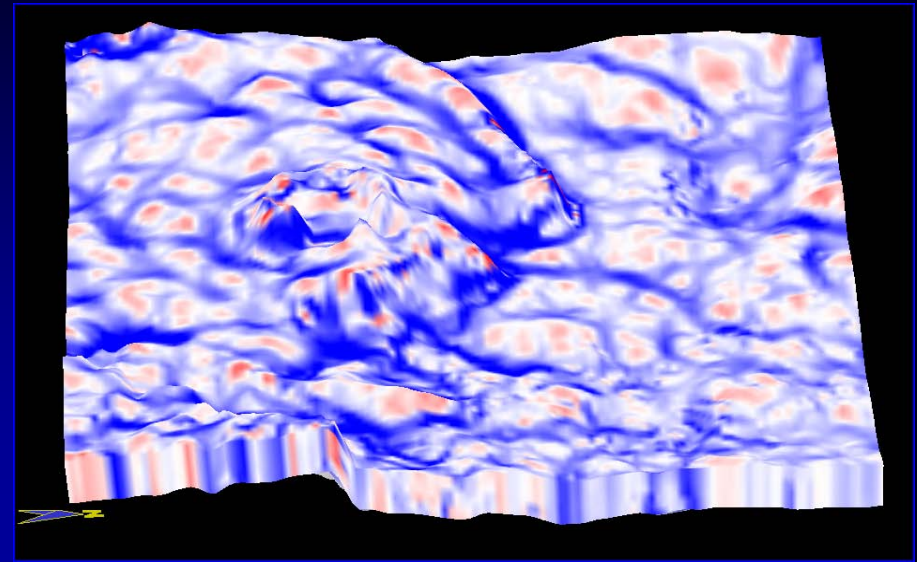


Strat-cube from most-negative curvature volume (low-res)

# Integration of coherence and volumetric curvature images



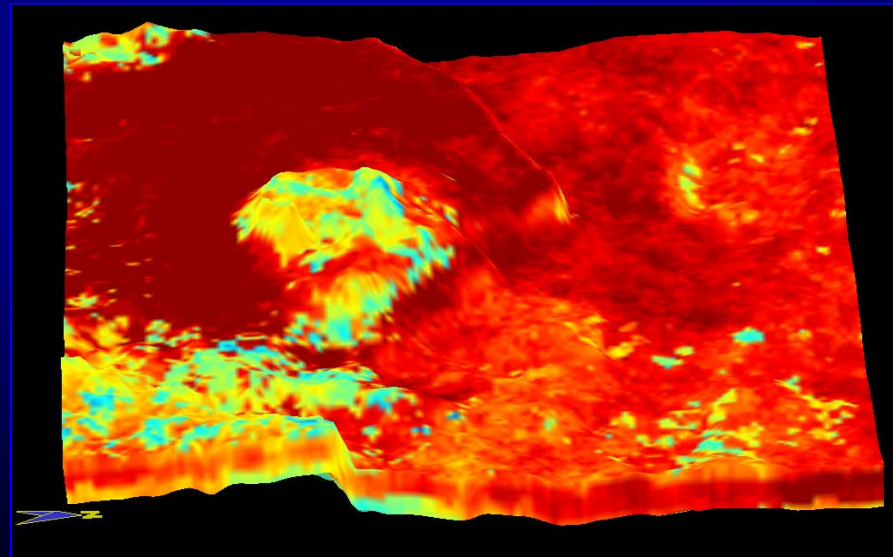
Strat-cube from most-positive curvature volume (high-res)

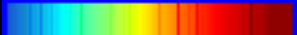


Strat-cube from most-negative curvature volume (high-res)

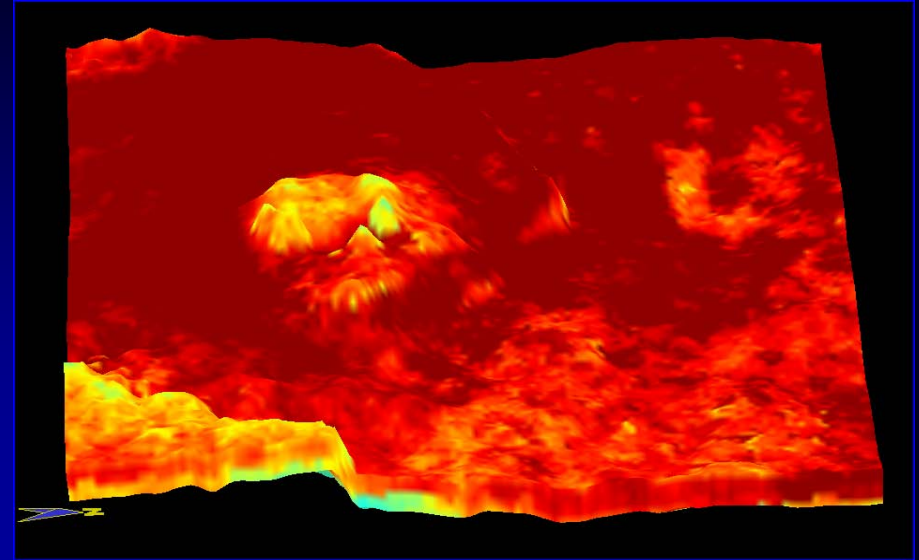
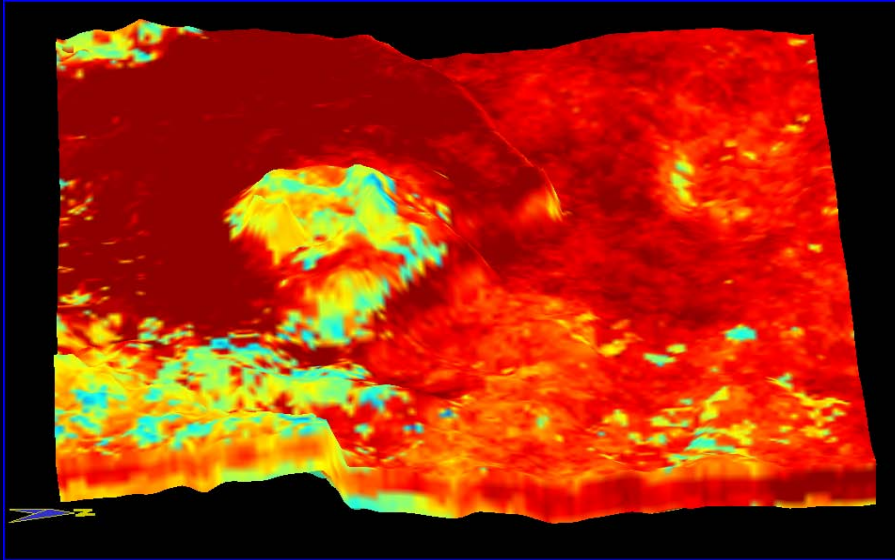
Low  High

Strat-cube from relative acoustic impedance volume



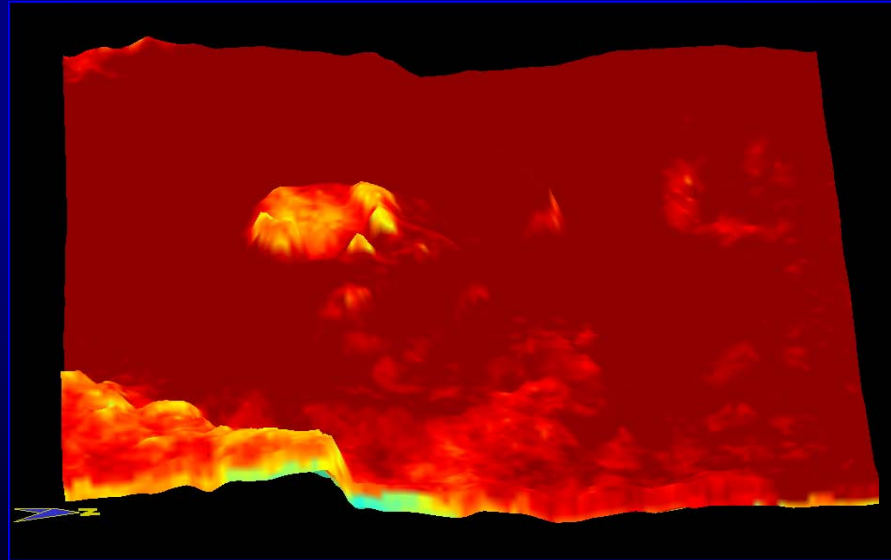
Low  High

# Integration of coherence and volumetric curvature images



Low  High

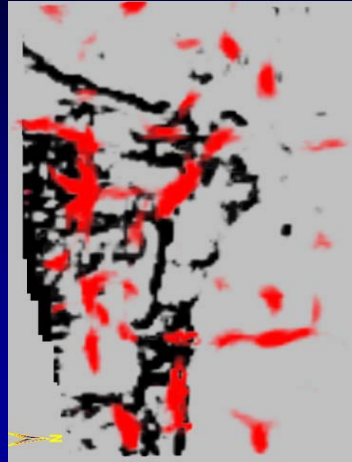
Strat-cube slices from relative  
acoustic impedance volume



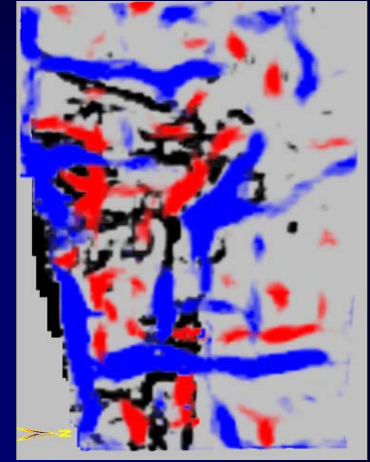
# Integration of coherence and volumetric curvature images



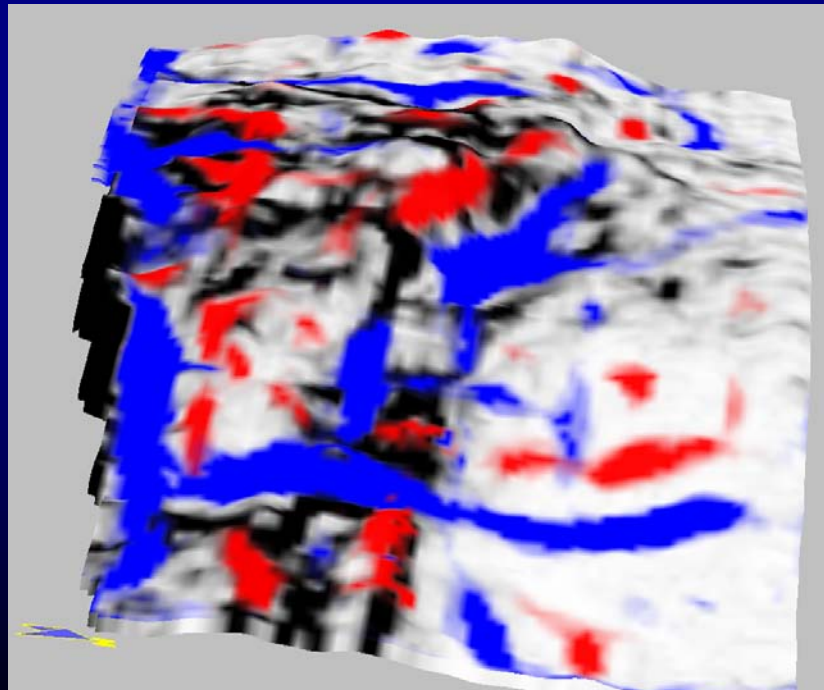
Coherence



Coherence +  $k_1$  curvature

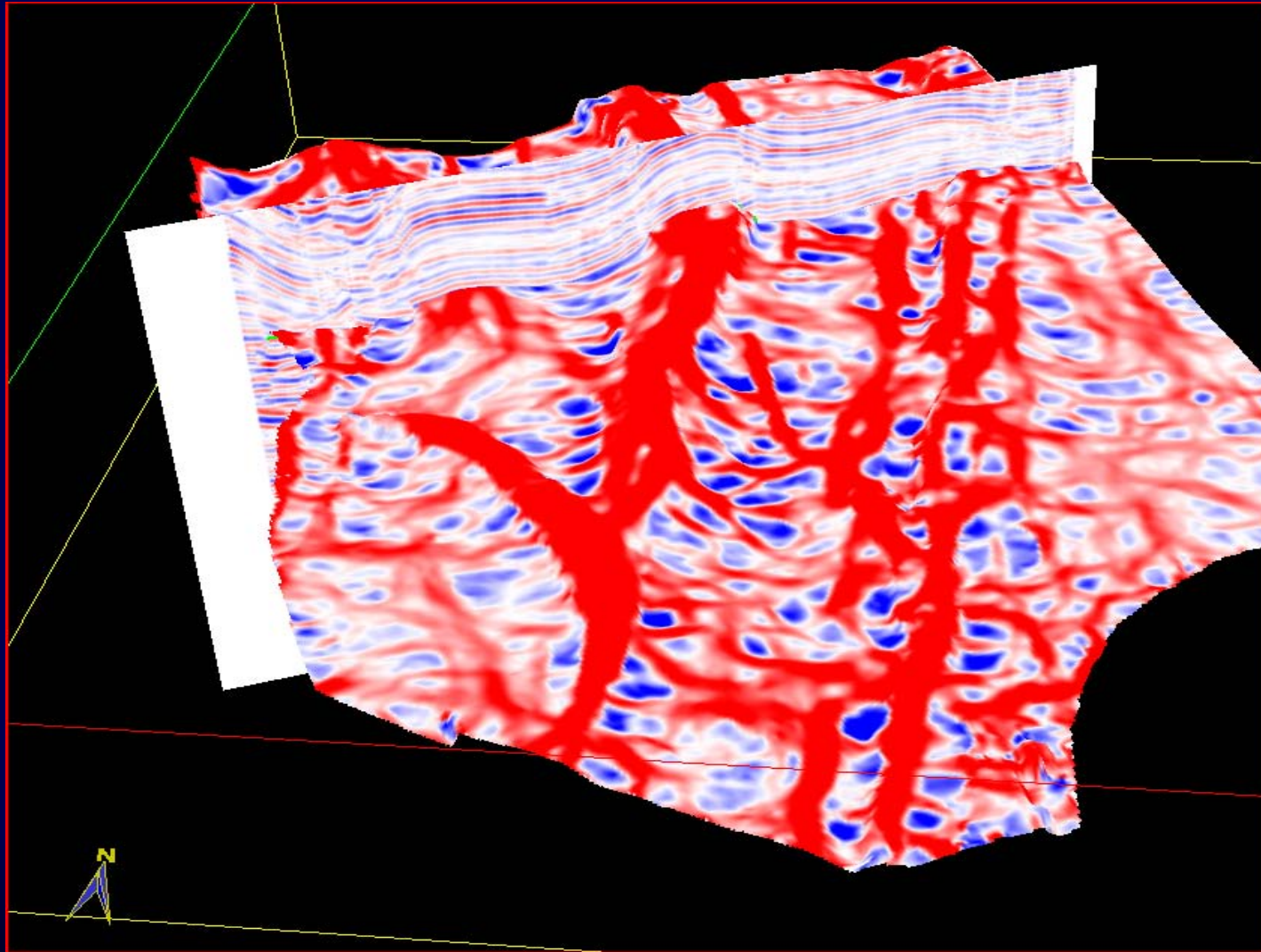


Coherence +  $k_1+k_2$  curvature



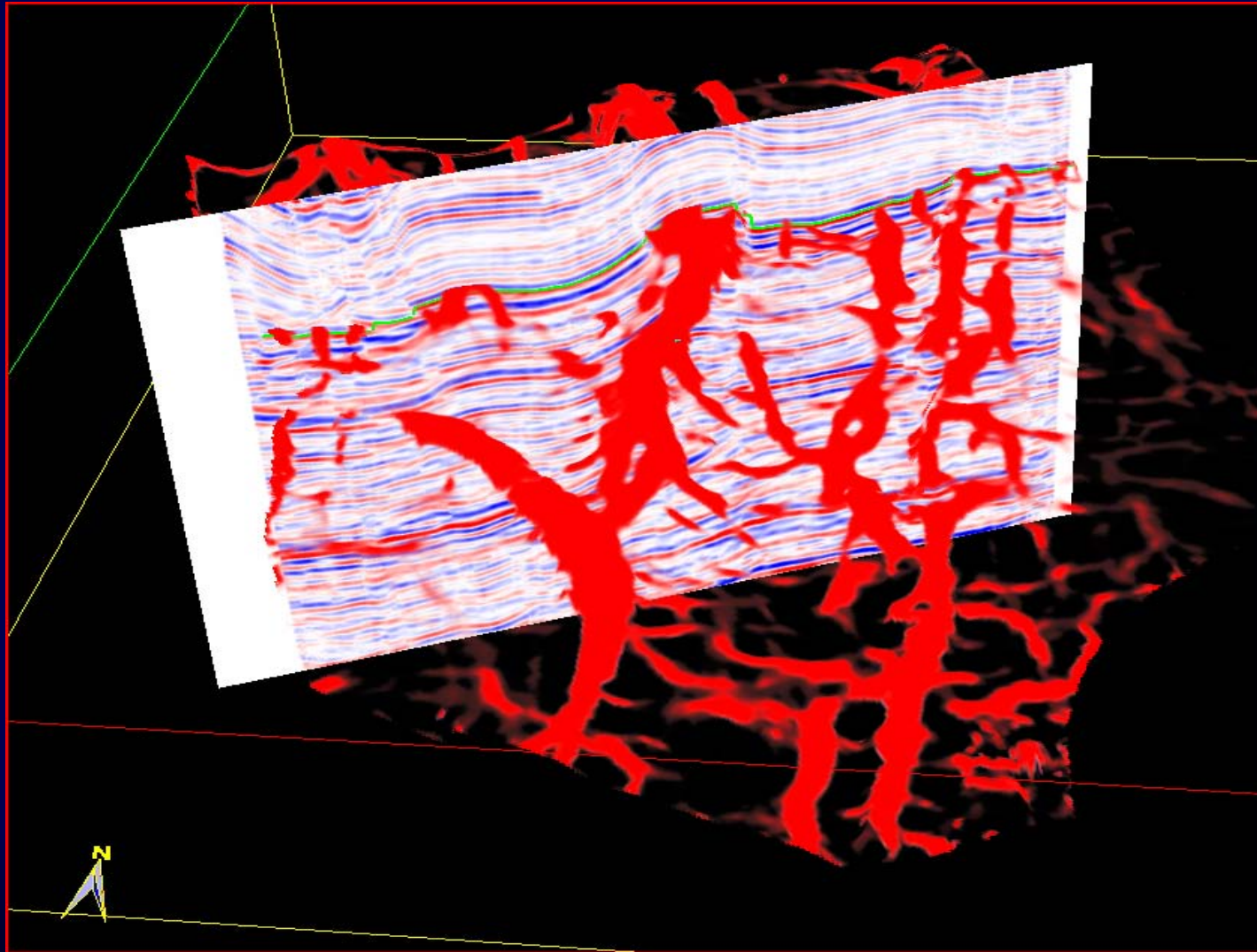
# Integration of coherence and volumetric curvature images

Multiattribute display using blending/transparency/opacity

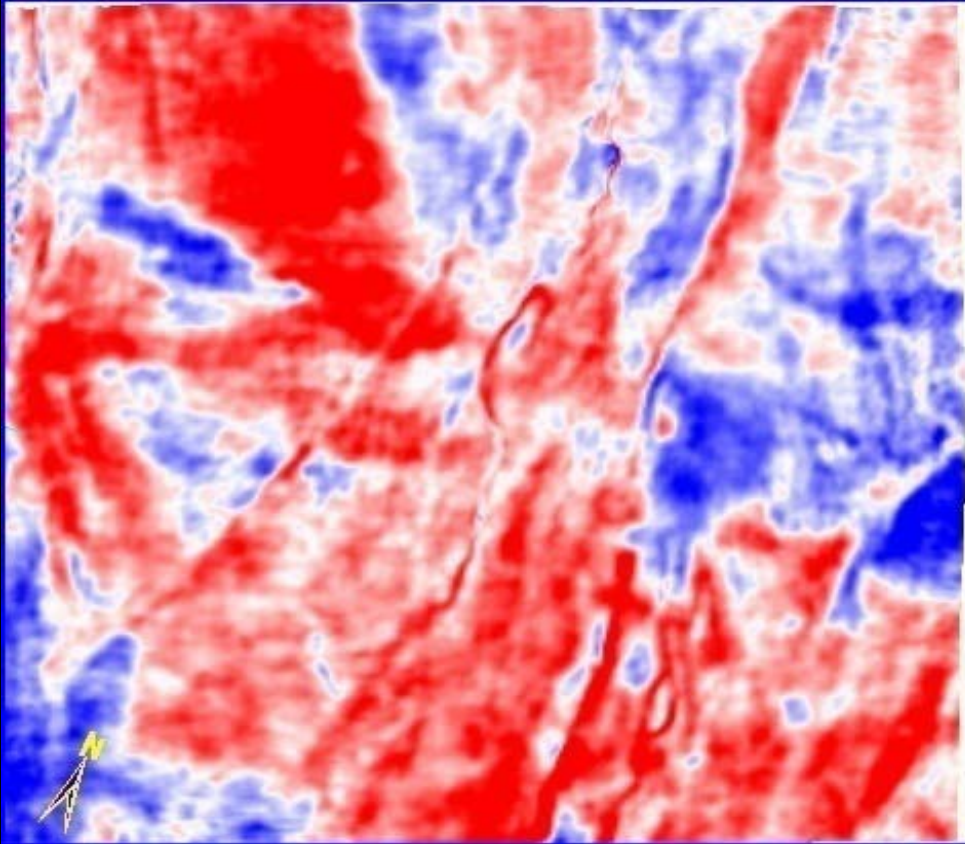


# Integration of coherence and volumetric curvature images

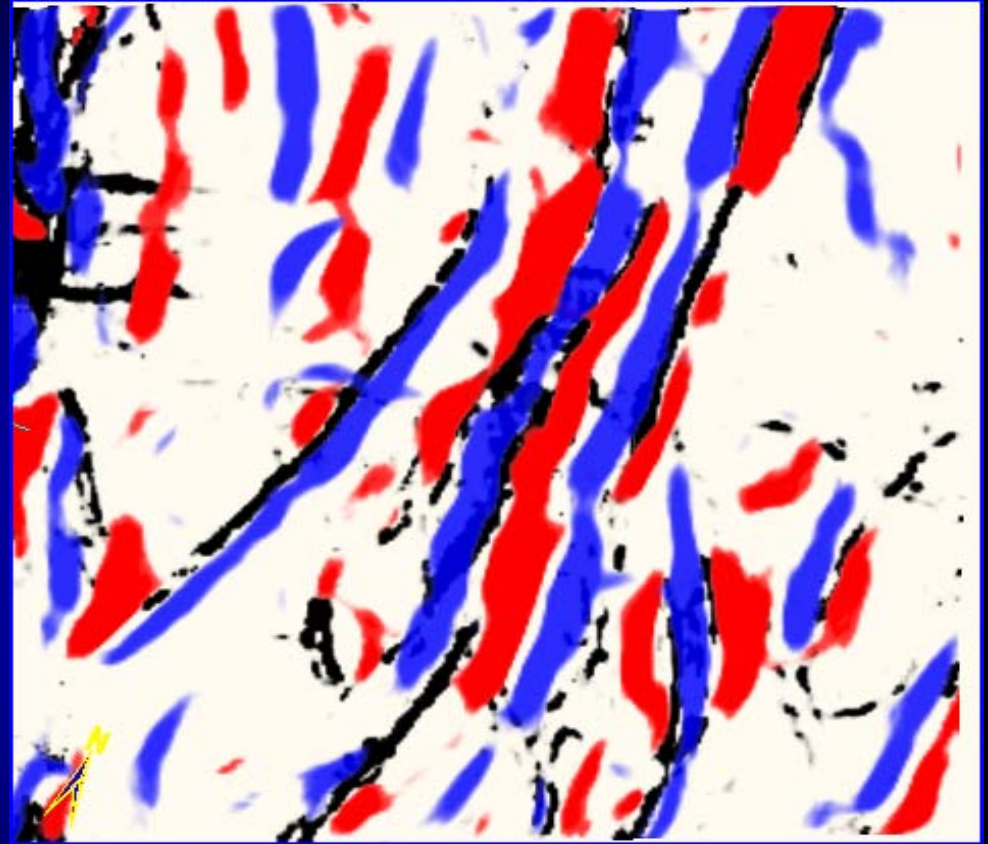
Multiattribute display using blending/transparency/opacity



# Multiattribute display using blending/transparency/opacity



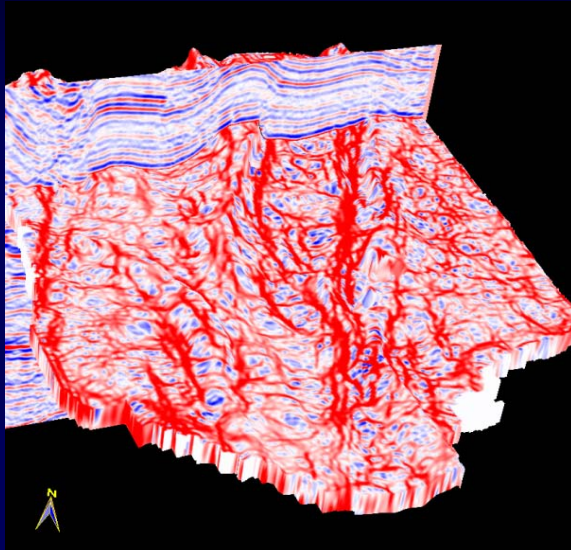
Horizon slice from input seismic data



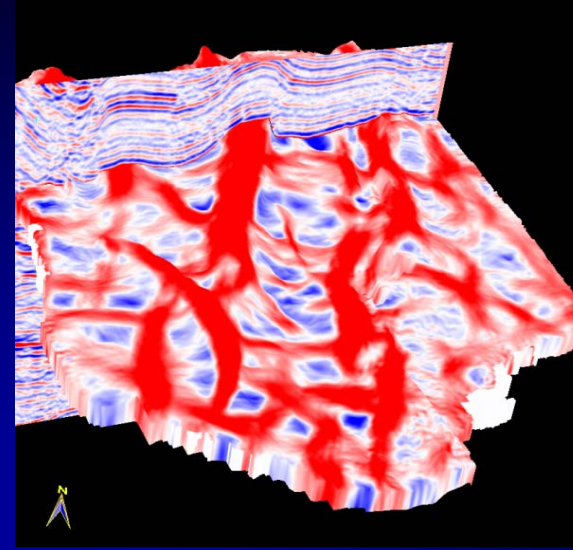
Horizon slice from merge of coherence (black), most-positive curvature (red) and most-negative curvature (blue) volumes. Transparency has been used to retain only the very low coherence values, the very-high positive curvature values and the very low negative curvature values.

# Structural curvature versus amplitude curvature

Strat-slice from  
amplitude most-pos  
curvature (LW)

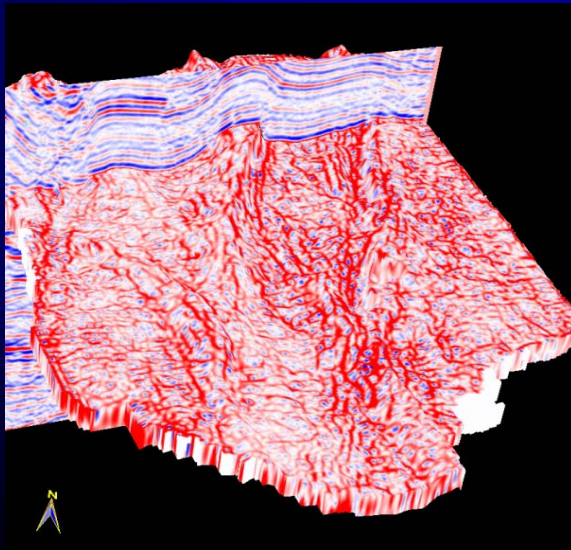


Strat-slice from  
structural most-pos  
curvature (LW)

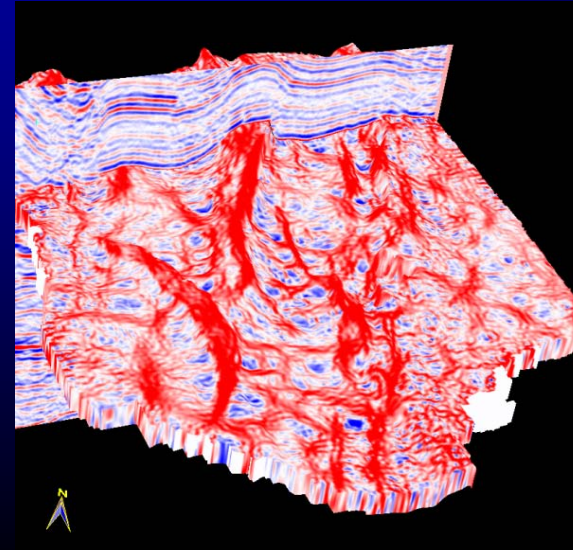


Low  High

Strat-slice from  
amplitude most-pos  
curvature (SW)

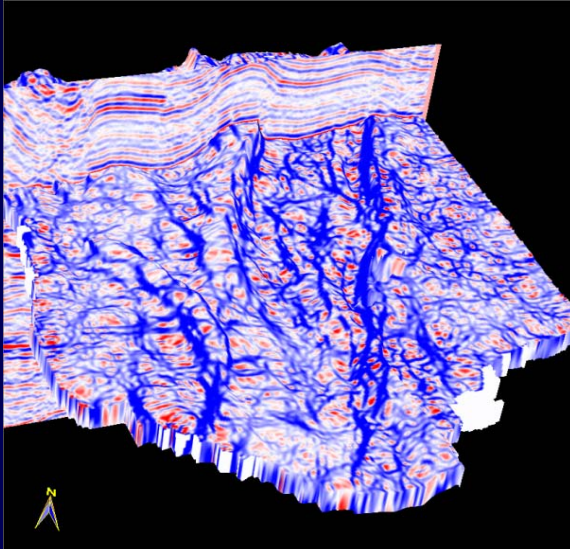


Strat-slice from  
structural most-pos  
curvature (SW)

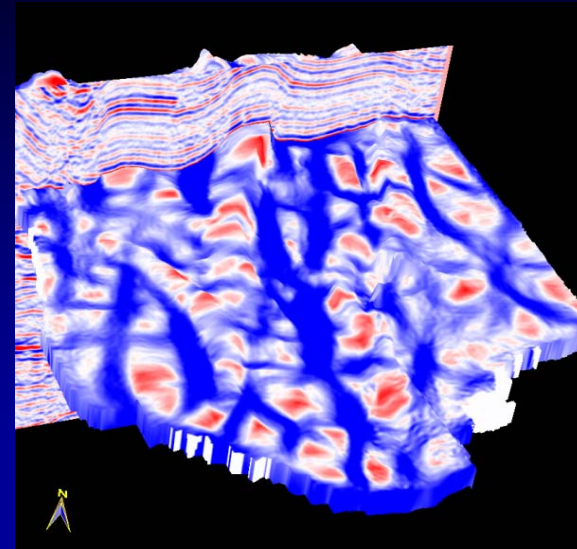


# Structural curvature versus amplitude curvature

Strat-slice from  
amplitude most-neg  
curvature (LW)

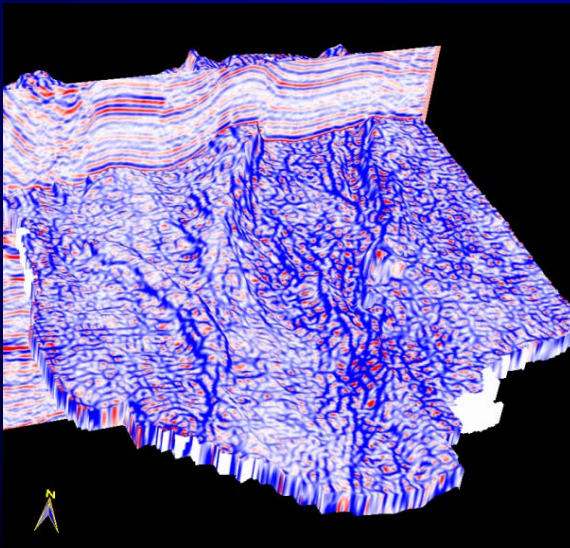


Strat-slice from  
structural most-neg  
curvature (LW)

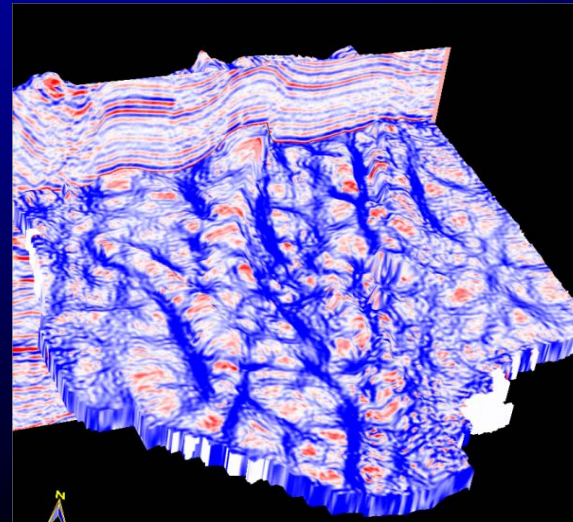


Low |  High

Strat-slice from  
amplitude most-neg  
curvature (SW)

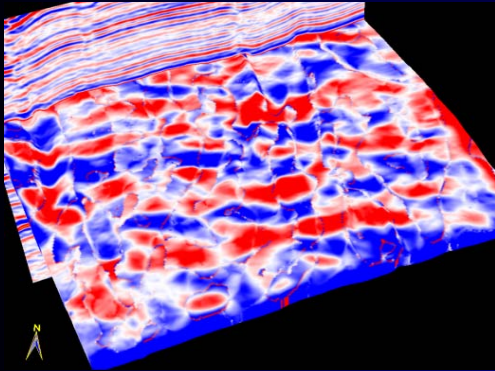


Strat-slice from  
structural most-neg  
curvature (SW)

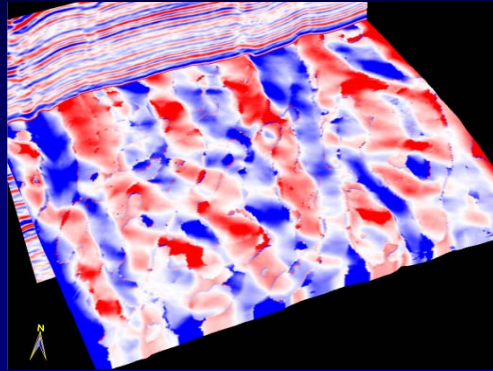


# Euler or azimuthal curvature

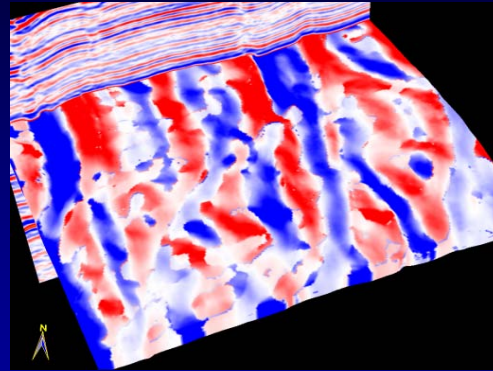
0 degrees



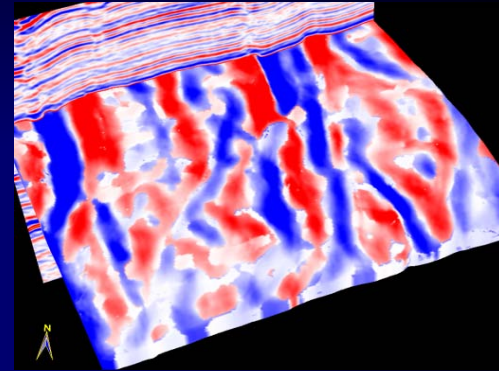
45 degrees



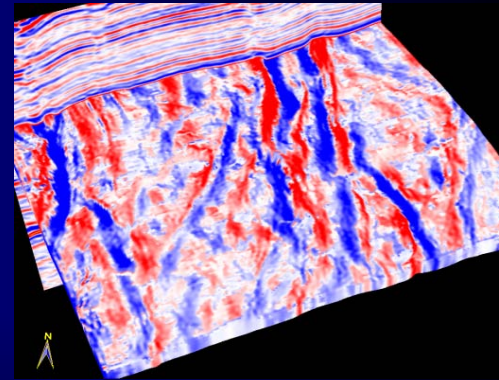
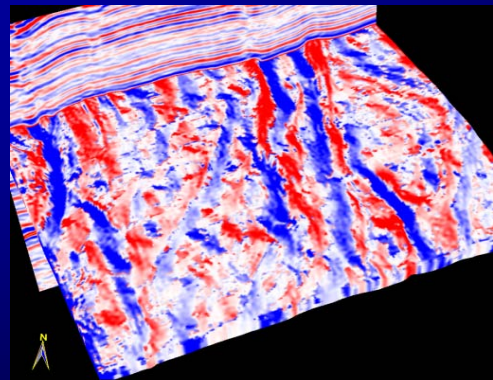
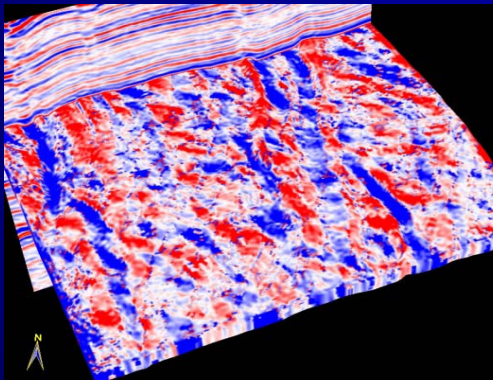
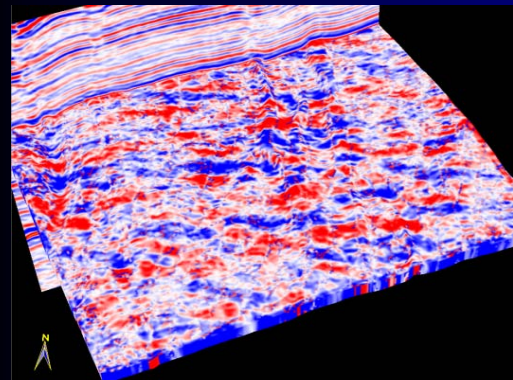
90 degrees



135 degrees

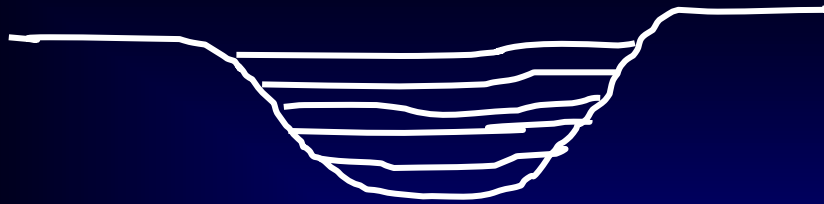


Long-wavelength

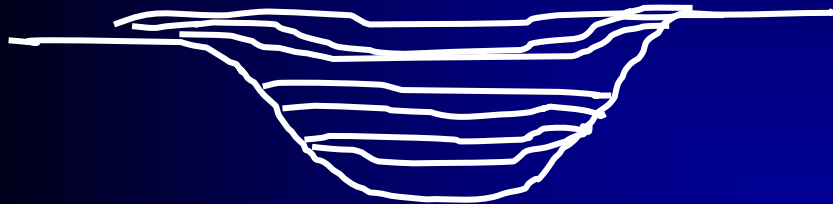


Short-wavelength

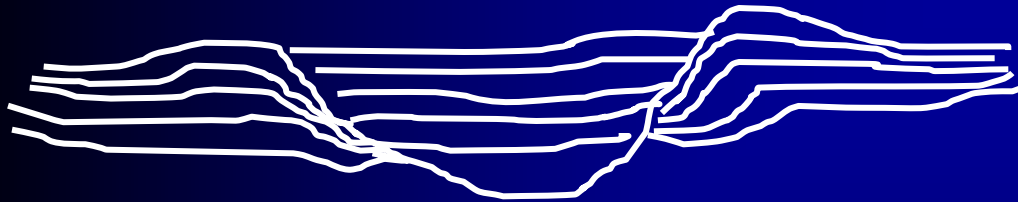
# Convergence within a channel with or without Levee/overbank deposit



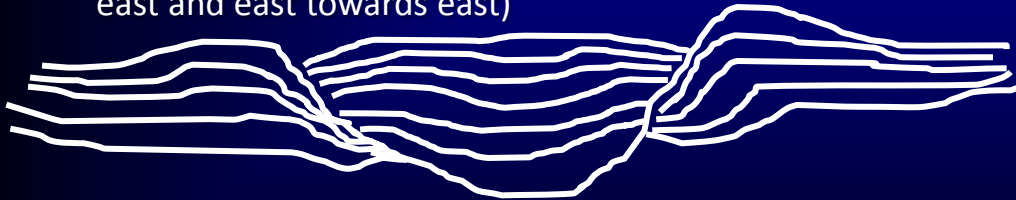
Case 1: No Significant convergence



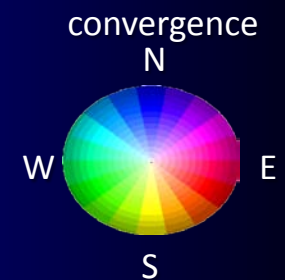
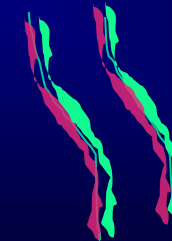
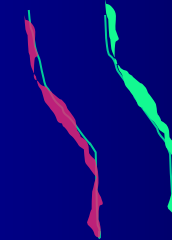
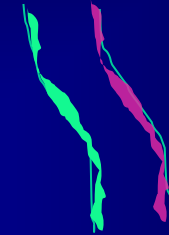
Case 2: Strata within channel: In west Channel margin converging towards west; In east channel margin converging towards east.

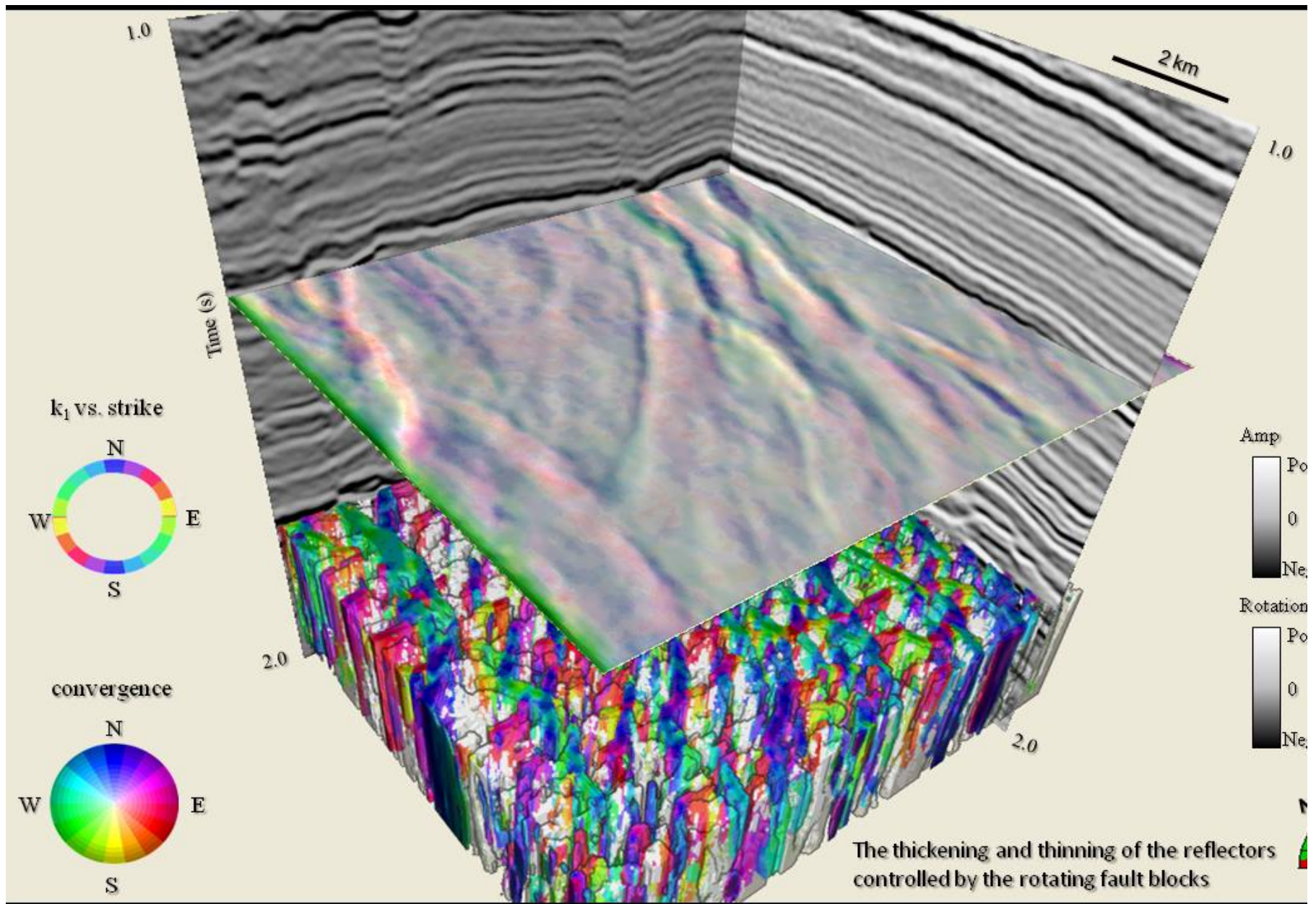


Case 3: Deposit within channel not converging at margin; but levee/overbank deposit converging towards channel ( west towards east and east towards east)

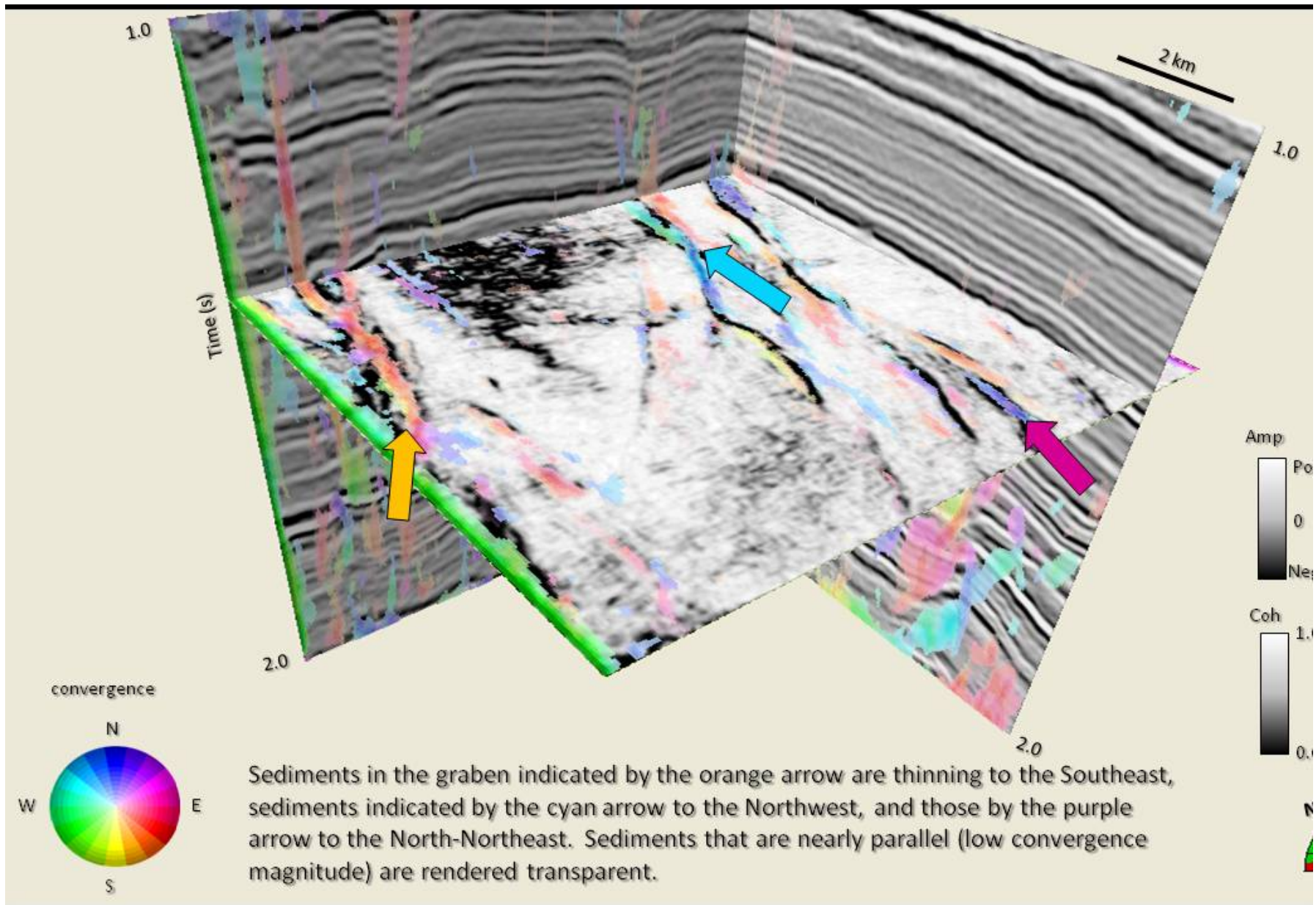


Case 4: Combination of Case2,Case 3 (both strata within channel and levee/ overbank deposit converging

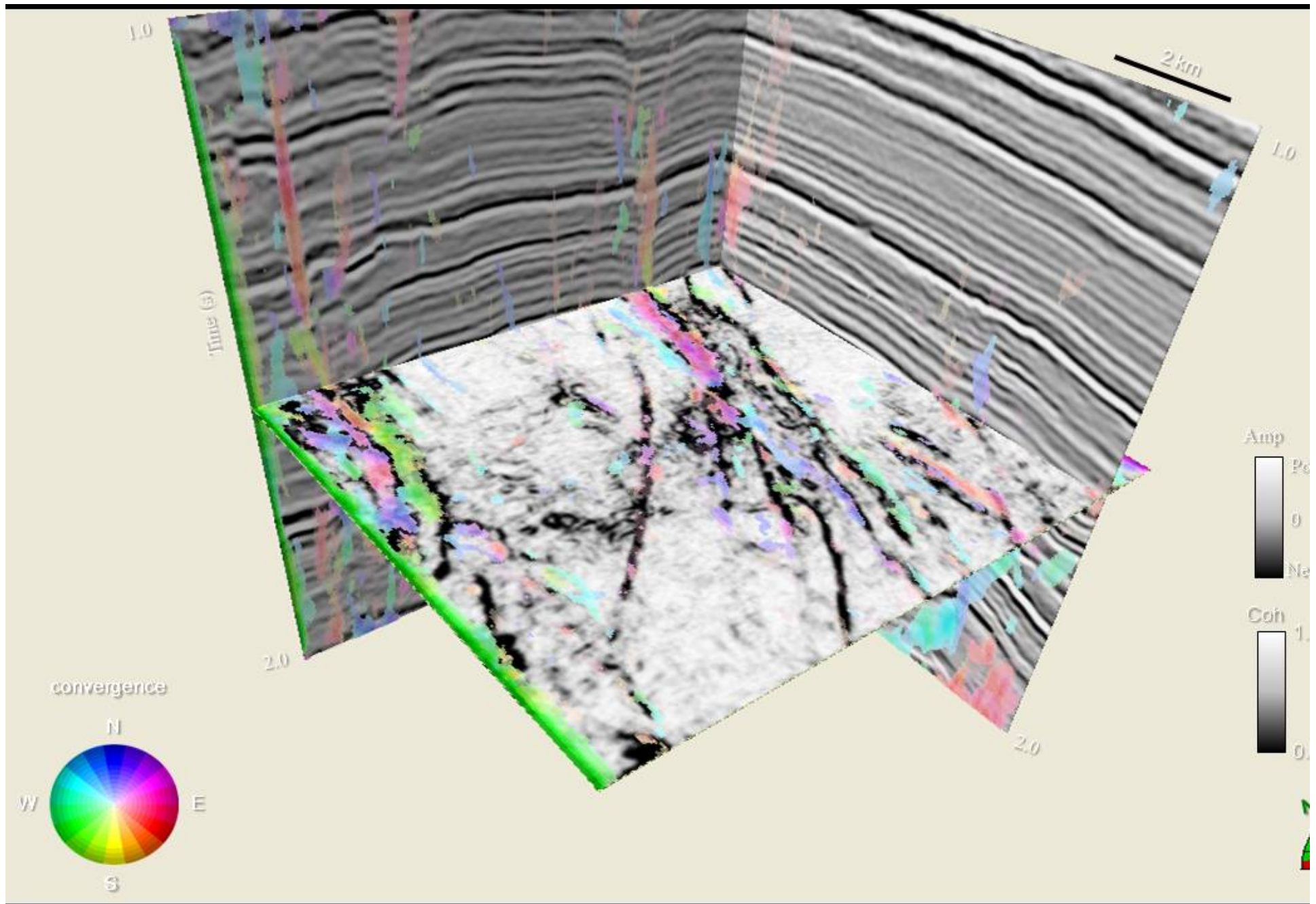




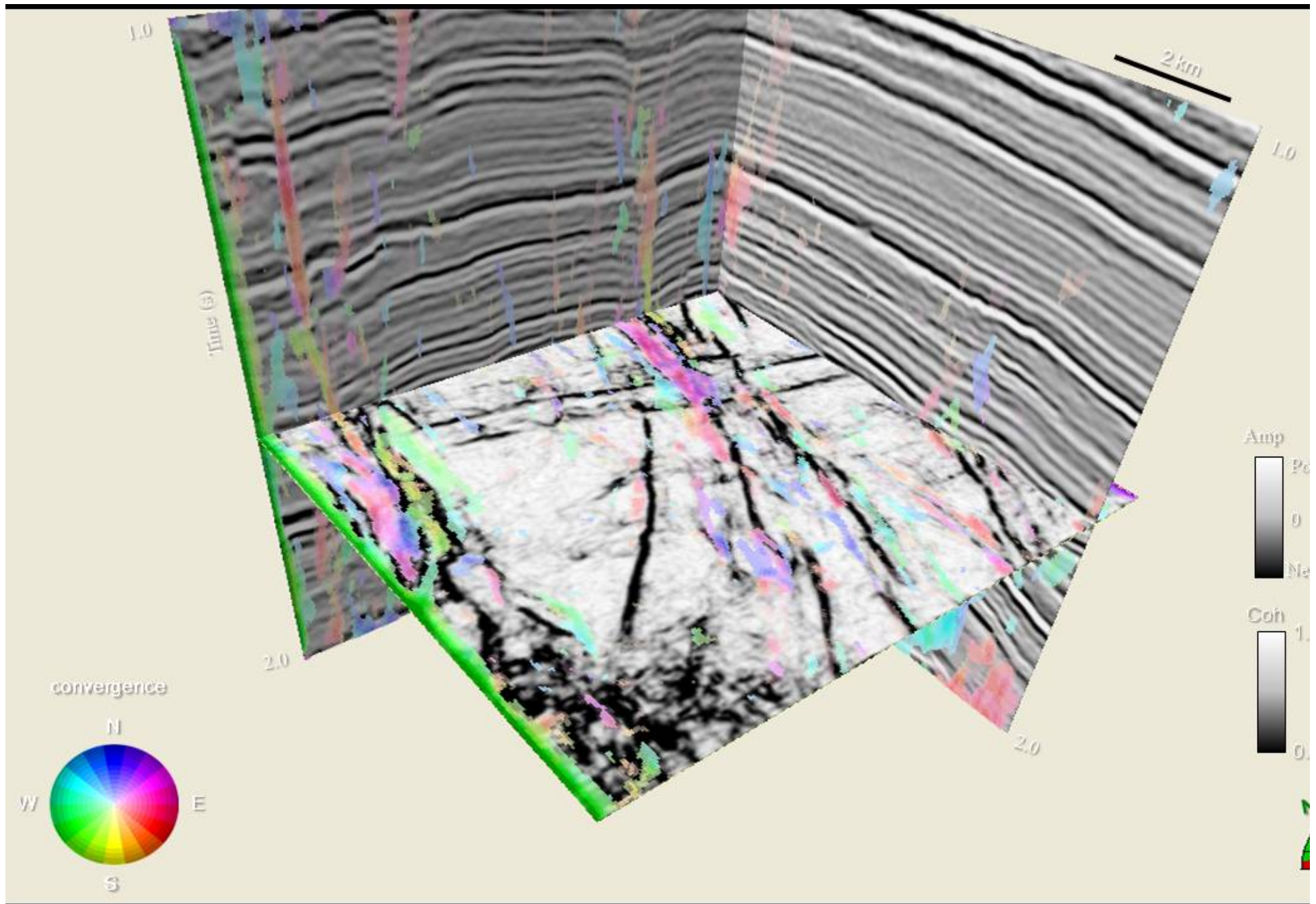
Notes by Presenter: Time slice at  $t=1.330$  s through a co-rendered image of reflector convergence displayed using a 2D color wheel and reflector rotation displayed using a gray scale and 50% transparency. We interpret the thickening and thinning of the reflectors to be controlled by the rotating fault blocks.



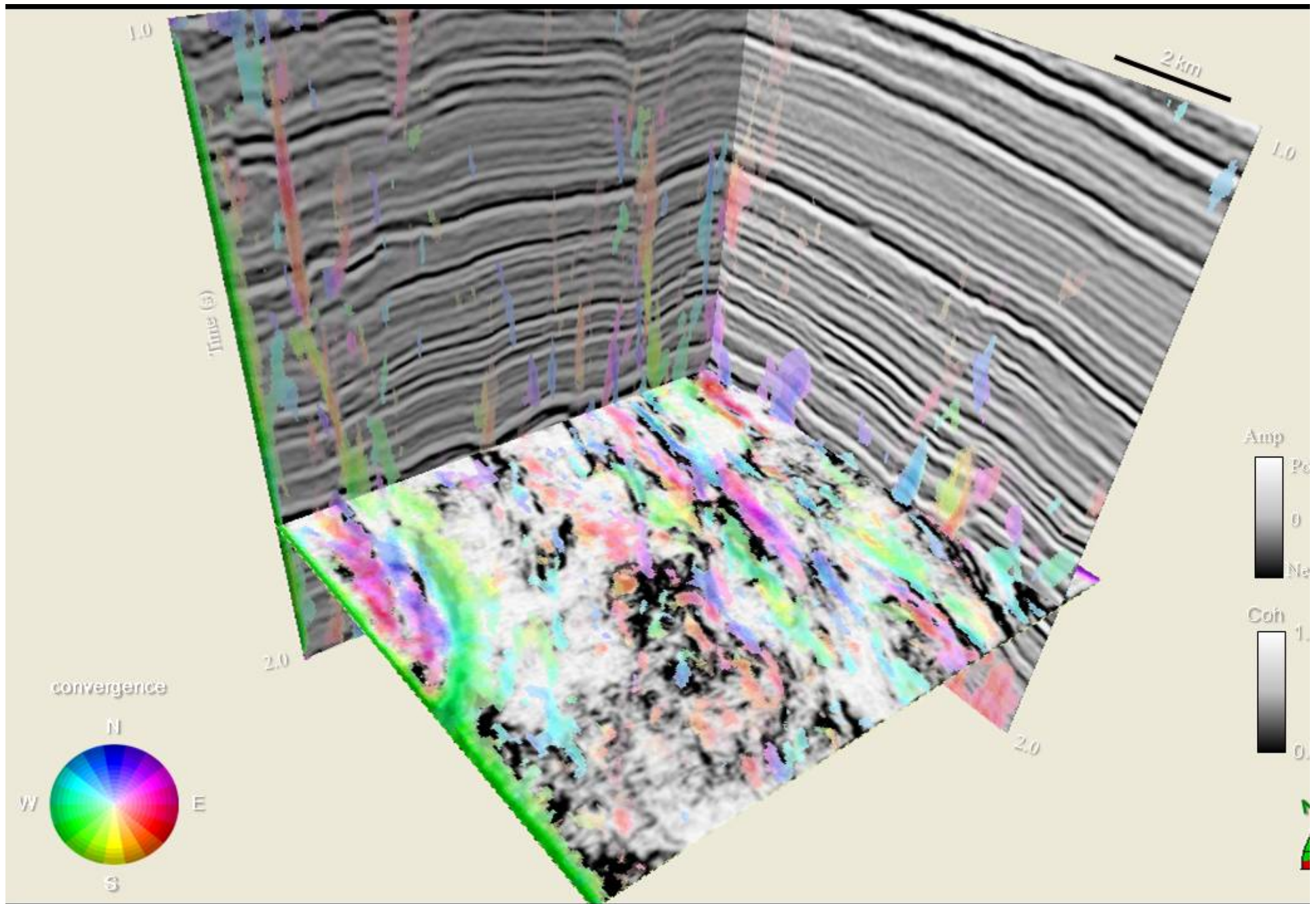
Notes by Presenter: Time slice at  $t=1.330$  s through coherence rendered against a gray-scale and reflector convergence displayed against a 2D color wheel. Sediments in the graben indicated by the orange arrow are thinning to the Southeast, sediments indicated by the cyan arrow to the Northwest, and those by the purple arrow to the North-Northeast. Sediments that are nearly parallel (low convergence magnitude) are rendered transparent.



Notes by Presenter: Time slice at  $t=1.500$  s through coherence rendered against a gray-scale and reflector convergence displayed against a 2D color wheel.



Notes by Presenter: Time slice at  $t=1.550$  s through coherence rendered against a gray-scale and reflector convergence displayed against a 2D color wheel.



Notes by Presenter: Time slice at  $t=1.710$  s through coherence rendered against a gray-scale and reflector convergence displayed against a 2D color wheel.

## Conclusions

1. We find that the principal curvatures  $k_1$  and  $k_2$ , where  $k_1 \geq k_2$ , provide the simplicity of interpretation seen in  $k_{pos}$  and  $k_{neg}$ , but retain the robustness of  $k_{max}$  and  $k_{min}$  in the presence of steep dip.
2. Multispectral volumetric curvature attributes are valuable for prediction of fracture lineaments in deformed strata.
3. Co-rendering volumetric curvature with coherence provides a particularly powerful interpretation tool.

## Acknowledgements

1. Arcis Corporation
2. Geomodeling Technology Corporation